Evaluating the Impact of Preparation Method on the Performance of Metal-Oxide Catalyst for Ethyl Mercaptan Removal from Natural Gas

Samuel Antwi , William Holmes , Dongmei Cao , Dhan Fortela , Tolga Karsili , Emmanuel Revellame , August Gallo , Mark E. Zappi , Rafael Hernandez *

Posted Date: 9 April 2026

doi: 10.20944/preprints202604.0621.v1

Keywords: sulfur compound; transition-metal; metal oxides; catalyst synthesis; adsorption; breakthrough time; impregnation; evaporation; filtration; natural gas

 doi:10.20944/preprints202604.0621.v1

Article

Evaluating the Impact of Preparation Method on the Performance of Metal-Oxide Catalyst for Ethyl Mercaptan Removal from Natural Gas

Samuel Antwi [1], William Holmes [1], Dongmei Cao [2], Dhan Fortela [1], Tolga Karsili [1], Emmanuel Revellame [1], August Gallo [1], Mark E. Zappi [1] and Rafael Hernandez [1,*]

[1] Chemical Engineering, Energy Institute of Louisiana, University of Louisiana at Lafayette, Lafayette, LA 70504, USA

[2] Advanced Microscopy and Analytical Core, Louisiana State University, Baton Rouge, LA 70803, USA

* Correspondence: rafael.hernandez@louisiana.edu

Abstract

The presence of toxic, corrosive, and environmentally harmful sulfur compounds within natural gas streams necessitates their removal to ensure compliance with fuel quality standards and regulations. Previous studies into MMOs (mixed metal oxides) as adsorbent or catalysts for sulfur compound removal have generally focused upon hydrogen sulfide (H_2S); however, few studies have assessed the removal of organic sulfur compounds like mercaptans. The purpose of this research is to investigate the effects of various preparation routes on the performance of supported metal-oxide catalysts that remove mercaptans from natural gases; specifically, filtration-based and evaporative based catalyst synthesis methods were investigated. A set of different catalysts; Mn, Cu, Zn, Ni and a composite (Mn-Cu-Zn-Ni) were prepared using filtration or evaporation solvent removal in this research and characterized by BET, FTIR, XRD, SEM, EDS and XPS, and their adsorption performance was assessed through fixed-bed breakthrough experiments under representative operating conditions (25°C, 200 psi, 36 mL/min). The results demonstrate that catalysts prepared via evaporation consistently exhibit greater sulfur compounds adsorption performance compared to catalysts prepared through filtration method, primarily due to enhanced retention of active metal species and improved surface accessibility. As confirmed from the characterization, all these improvements result from the fact that the evaporation method enhances the interaction between the metals and oxygen (FTIR); increases the amount of oxides formed as well as improves their distribution (XRD); provides access to more available metal surfaces (XPS/EDS); and creates pore structures and morphologies that are more open and accessible (SEM/BET). Among the catalysts studied, the Mn and Cu catalysts prepared by evaporation achieved the highest breakthrough times 1410 minutes and 1350 minutes, respectively, exceeding the performance of a commercial benchmark catalyst with breakthrough time of 1200 minutes under identical conditions. These findings demonstrate that the evaporation method enables more effective utilization of metal-oxygen active sites and significantly enhances sulfur adsorption capacity. Overall, this work establishes evaporation as a superior and scalable preparation strategy for metal oxide catalysts and provides important structure performance insights for the design of cost-effective catalyst for industrial natural gas desulfurization, particularly for the removal of organic sulfur compounds from natural gas.

Keywords: sulfur compound; transition-metal; metal oxides; catalyst synthesis; adsorption; breakthrough time; impregnation; evaporation; filtration; natural gas

1. Introduction

Sulfur compounds in a natural gas stream represent problems of toxicity, corrosion, odor, and harm to equipment downstream. Sulfur compounds could also act as poisons for catalysts used for

 doi:10.20944/preprints202604.0621.v1

direct or indirect conversion of methane into fuels and chemicals. The removal of sulfur compounds is required by specifications on fuel quality, process safety, and environmental regulations. Mercaptans are particularly troublesome among all sulfur containing species as their selective removal from a feedstock can be difficult and they may still be present in amounts that exceed specified limits even after reduction of other sulfur species to acceptably low levels [reference]. In particular, organic sulfur compounds are of interest due to their presence in gas systems and the high degree of affinity these species exhibit with active surface sites making them ideal model compound for studying adsorbent or catalyst activity toward natural gas treatment [1–3].

Metal oxides (MO) are being researched as potential catalysts or adsorbent materials for removing sulfur from gas streams. They present various advantages over other adsorbing materials including a large number of active redox and adsorptive sites on the surface, and they may also have variable compositions at lower costs than many adsorbing materials. Many transition metal oxides such as those containing Mn, Cu, Zn, or Ni have been studied for sulfur capture based upon the interactions that occur between these oxides and sulfur-based molecules. These include chemisorption, metal-sulfur affinity and surface oxygen species. Most studies conducted using MOs for sulfur removal have focused on H_2S removal rather than organic sulfur compounds, which are important when considering the use of MMOs in industrial gas treatment processes [4,5].

The efficiency of a catalytic reaction in a metal-oxide supported system depends upon how well the active phase of the metal is stabilized and dispersed on the surface of the support. Because of this dependence, the method used to prepare the catalyst can be just as or even more important than the composition of the catalyst. The method of synthesizing a catalyst will ultimately determine the chemical properties of its surface, how easily it can access pores within its structure, whether oxides develop during exposure to air, and where active sites are located on its surface, all of these factors influence an increase in adsorption activity. Of many different synthesis techniques that have been developed for supported catalysts, impregnation-based routes are among the simplest and most cost-effective methods available to researchers and industry personnel for preparing catalysts due to their versatility [6–8].

The process of removing solvents during catalyst preparation is an essential and commonly overlooked part of the overall preparation process. During the solvent removal stage, there are many factors to consider such as redistribution of dissolved precursors within a support by virtue of capillary flow, diffusion, adsorption-desorption and/or local supersaturation effects. These factors can greatly affect if a synthesized catalyst will exhibit uniformly dispersed active oxides or suffer from metal loss, poor dispersion, or uneven surface coverage. The most commonly used method for solvent removal is filtration. Filtration involves separating the solid from the liquid phase prior to completing solvent removal. Consequently, some dissolved precursor species may be lost with filtrate. This work introduces evaporation, which involves gradually removing the solvent from the solution while continuously exposing the solution to the support. Therefore, all soluble precursor species have time to deposit and develop into an oxide structure prior to calcination. This distinction is significant since the performance of a supported catalyst is not solely dependent upon the total amount of metal present, but also upon how much of it remains available as accessible surface-bound metal-oxygen reactive sites following synthesis [7–9].

Although it is well understood that both drying and precursor redistribution are important to catalyst preparation, there has been relatively little research into the impact of removing the solvent from the system on adsorption properties of the sulfur compound being removed. Most of the research has focused on the composition of the catalyst; the effect of promoters, etc.; or the adsorption capacity of the catalyst. Very few studies have made systematic observations as to whether changing the method of preparation will result in changes to metal retention, oxide formation, pore accessibility and sulfur breakthrough. As such this lack of understanding is especially relevant when considering the development of low cost, high volume adsorbent catalysts.

The research in this study utilized a series of supported metal oxides formed over a halloysite support by two solvent removal methods: filtration and evaporation. These removal methods are to

 doi:10.20944/preprints202604.0621.v1

compare the effects of both solvent removal methods on the adsorption of sulfur compounds from natural gas. Halloysite is an attractive candidate as a support due to its aluminosilicate structure with high density of surface hydroxyl groups and ability to deposit metal oxides [10]. Four single-metal catalysts of Mn, Cu, Zn, and Ni, along with one composite (Mn-Cu-Zn-Ni), were produced and analyzed via BET, FTIR, XRD, SEM, EDS, and XPS. Following characterization of each catalyst their sulfur adsorption performance was evaluated using a fixed bed reactor at representative process conditions.

This research aims to identify the effects that filtration and evaporation have on the ability of the MO catalysts supported by halloysite to remove sulfur compounds from natural gas; also, the extent to which these processes affect active metal retention, oxide formation, surface availability and breakthrough characteristics. This research establishes a link between the synthesis method used and the structure of the catalyst and adsorption properties to better understand how various synthesis parameters can be controlled to enhance the catalytic activity of adsorbers and show the feasibility of using evaporation as an economical, scalable, industrial process to develop high-performance adsorbent materials for desulfurizing natural gas.

2. Results and Discussion

2.1. The Analysis of Surface Morphology of the Prepared Catalyst

2.1.1. The Analysis of BET Data of Filtration vs Evaporation Prepared Catalyst

The BET textural characteristics of the single-metal and composite catalysts synthesized using evaporation and filtration as shown in **Table 1** demonstrate that the method used to remove solvents has a significant effect on the ultimate structure of the catalysts including their surface area, pore volume, and pore size. These three structural characteristics are key factors in determining adsorption capacity for sulfur removal as well as the number of available catalytic sites and the ability of sulfur compounds to diffuse to internal surfaces within porous adsorbent and supported catalyst structures [18,19].

Table 1. BET Data of Catalyst Prepared via Filtration vs Evaporation Method.

	Filtration Method			**Evaporation Method**		
Catalyst	Surface Area Cm^2/g	Pore Volume cm^3/g	Pore Size Å	Surface Area cm^2/g	Pore Volume cm^3/g	Pore Size Å
Manganese	10.833	0.091	278.592	43.308	0.223	173.019
Copper	9.651	0.076	267.470	18.292	0.125	239.067
Zinc	38.769	0.213	187.902	14.034	0.096	274.758
Nickel	40.218	0.201	165.525	23.405	0.118	222.430
Composite	21.783	0.096	172.030	17.717	0.133	241.840

A clear pattern exists for both the manganese and copper samples prepared using the two methods of preparation: the evaporated samples had significantly larger surface areas and pore volumes than those that were prepared via filtration. The surface area of Mn was doubled when it went from a surface area of 10.833 m^2/g to 43.308 m^2/g. The pore volume also increased. It went from a pore volume of 0.091 cm^3/g to a pore volume of 0.223 cm^3/g. Similar increases occurred in the surface area and pore volume of Cu. The surface area increased by nearly double from 9.651 m^2/g to 18.292 m^2/g, and the pore volume increased by almost a factor of 2 from 0.076 cm^3/g to 0.125 cm^3/g. These findings suggest that the slowest rate of solvent loss occurs when solvents are removed by

 doi:10.20944/preprints202604.0621.v1

evaporation, which allows for a more developed network of pores and an improved accessibility of the interior surface. This phenomenon has been observed previously, where researchers have shown that slower rates of solvent loss promote more uniform distribution of precursors within porous materials and reduces the amount of structural collapse occurring during the transition from liquid to solid state [7,9,20].

In contrast, Zinc and Nickel catalysts showed an inverse relationship to the method of preparation, filtration being used to prepare catalysts resulted in higher surface areas and pore volumes compared to using evaporation. The surface area and pore volume of Zn both were reduced significantly upon use of the evaporation method. The surface area of Zn decreased by approximately 64% (from 38.769 m^2/g to 14.034 m^2/g) and the surface area of Ni decreased by approximately 42% (from 40.218 m^2/g to 23.405 m^2/g) due to use of the evaporation method, the same was true for the pore volume measurements. These results indicate that the effect of the method of preparation can be dependent on the specific metal and its interaction with the support material during precipitation and solidification. Evaporation may cause a greater degree of pore fillings or structural densification at the local scale as the metal oxides form into the supporting structure, thus resulting in lower measured surface area and less available pore volume. Variations in this type of behavior are typical for supported catalysts and depend heavily on the balance between pore formation and pore occupation as determined by precursor chemistry, metal loading, and drying conditions [6,21].

The average pore sizes presented in this paper also show how the structure of each material changed after evaporation. Evaporation produced a reduction in pore size for Cu, as evidenced by the measured slight reduction from 267.470 to 239.067Å. Zn, Ni, and the composite material showed increases in pore size, a significant increase from 187.902 to 274.758Å for Zn; an even greater increase from 165.525 to 222.430Å for Ni; and a moderate increase from 172.030 to 241.840Å for the composite material. Except for Cu, the pore size results indicate that the preferred result of evaporation was the generation of larger and thus more easily accessed mesopores (2-50 nm pores that enhance adsorbate diffusion and active-site accessibility). Even the Cu pores formed by evaporation are comparable to Zn, Ni, and the composite material. Larger and thus more easily accessed mesopores are beneficial for gas phase adsorption as they allow less resistance to diffusion of sulfur containing molecules through the pore space toward available active sites on the surface. Mn did not follow this pattern since its pore size actually decreased from 278.592 to 173.019Å with both surface area and pore volume showing significant increases. Thus, evaporation in the Mn catalyst appears to promote the formation of a higher density of smaller mesopores (2–50 nm), rather than fewer large pores, leading to improved surface accessibility as a result of the reduced average pore diameter. This pattern is similar to what would be expected when producing a finer divided pore network than would occur if pore size alone were being enlarged [19,22,23].

For the Mn-Cu-Zn-Ni composite catalyst, with respect to surface area, there was a modest decrease (21.783 m^2/g vs. 17.717 m^2/g) during transition from filtration to evaporation. Conversely, both the pore volume and pore diameters increased by 39% (0.096 cm^3/g vs. 0.133 cm^3/g) and 40% (172.03 Å vs. 241.84 Å), respectively. While the total surface area of the composite prepared through evaporation was marginally less, the increase in pore volume and pore diameters clearly indicates that the pores were more open and accessible than those produced using filtration. The greater porosity can lead to better breakthrough behavior than a minor increase in BET surface area alone since access to pores as well as diffusional resistance can dominate the use of available sites in adsorption/catalytic reactions involving gases [18,21,22]. Hence, the improvement in breakthrough behavior exhibited by the Mn-Cu-Zn-Ni composite prepared via evaporation is also reflected in an enhanced pore structure.

Overall, the BET data show that evaporation does not simply increase or decrease all textural parameters uniformly but instead alters the catalyst structure in a way that depends on the metal precursor system and its interaction with the support during drying. In general, evaporation tends to favor larger pore accessibility and better pore connectivity, while filtration more often yields denser structures with smaller accessible pore networks.

 doi:10.20944/preprints202604.0621.v1

2.1.2. XRD Analysis of Catalysts Prepared by Filtration vs Evaporation

The X-ray diffraction patterns have been evaluated as a means for determining whether there was an influence from the different preparation routes (i.e., filtration vs. evaporation) that affected the development of crystalline structure/phase, and the dispersion of the deposited metal oxides onto the halloysite support as shown in **Figure 1**. Comparisons can be made based upon the relative differences in peak intensity, peak width (sharpness), and peak definition which generally relate to crystallinity, oxide development and dispersion of the supported metal species. Generally, sharper and more intense peaks correspond to higher degrees of crystallinity and/or larger oxide domains. Conversely, broader peaks or those peaks that show lower intensities are indicative of smaller crystallite dimensions, greater metal species dispersion, and/or strong interactions between the metal species and the supporting material [6,21].

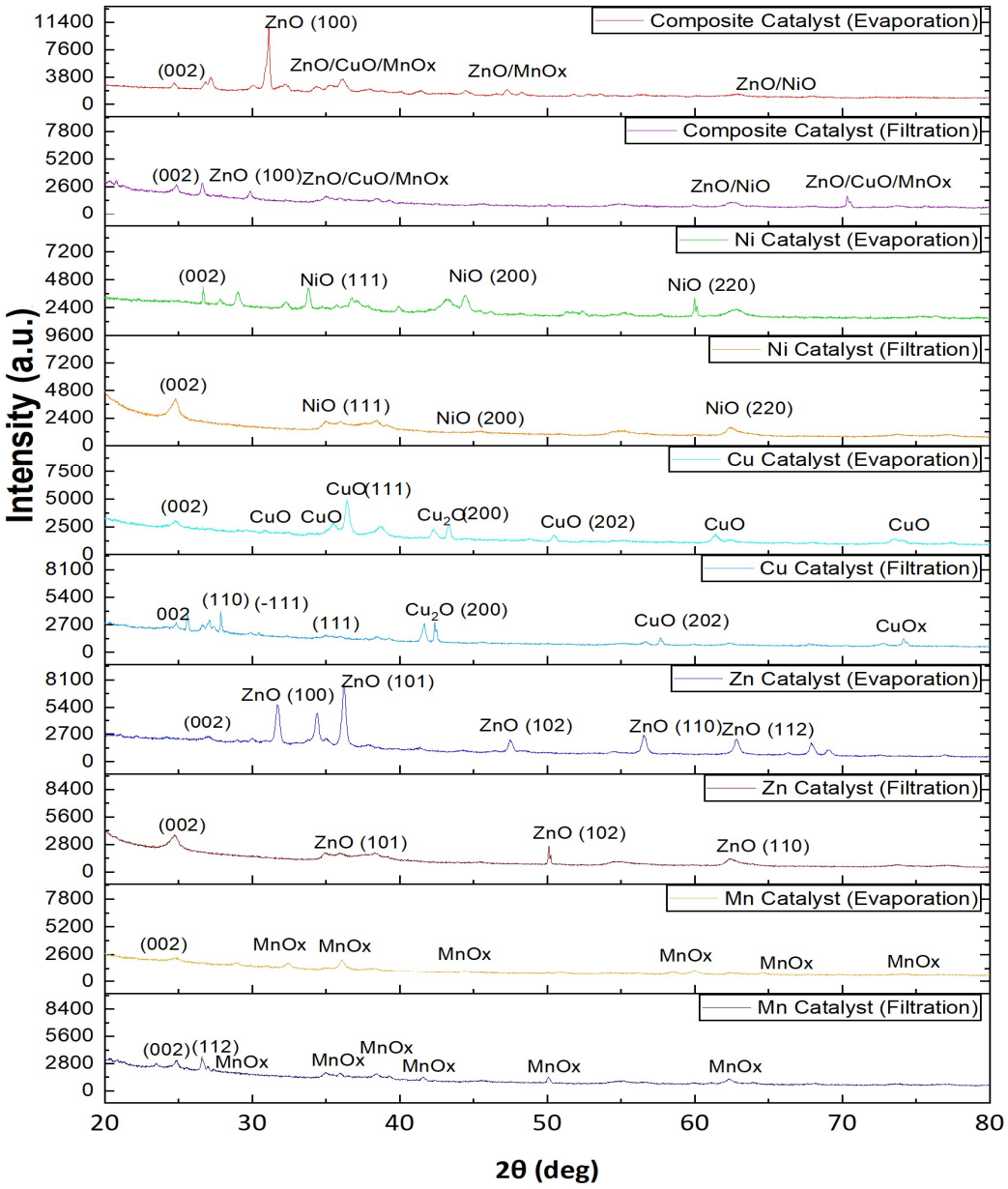

Figure 1. XRD Spectrum of the Catalysts.

 doi:10.20944/preprints202604.0621.v1

The peaks that were produced by the filtered Mn catalyst are found in a wide range, centered on 2θ = 28.9°, 32.3°, 36.1°, 44.4°, 50.8°, and 58.5-60.0°, which correspond to Mn_3O_4. These are associated with the (112), (103), (211), (220), (105), and (224)/(303) diffraction planes, respectively. In addition, a peak attributed to the halloysite (002) plane was located at approximately 2θ = 24.8°. Due to their breadth, however, it cannot be ruled out that peaks produced by Mn_2O_3 also exist (i.e., 32.9° (222), 38.2° (400)). Thus, the manganese phase can most reasonably be described as MnOx (Mn_3O_4/Mn_2O_3). In the evaporated Mn catalyst, the same MnOx-related reflections as in the filtered Mn catalyst were observed; however, they were much broader and less intense than those for Mn_3O_4 (103), and (211) respectively. The appearance of these reflections indicates that evaporation caused a reduction in the crystallite dimension of Mn-oxide and increased the dispersion of MnOx within the material. Therefore, although both methods created manganese oxides, there was a slight preference for Mn_3O_4 crystallites in the case of filtration versus a preferred dispersal of MnOx species with less long-range ordering when using evaporation.

The peaks in the diffractogram of the filtration prepared Cu catalyst match those expected for CuO. They appear at a Bragg angle of about 2θ = 32.5° (CuO(110)), 2θ = 35.5° (CuO(-111)) and 2θ = 38.7° (CuO(111)). There is also a small feature located close to a Bragg angle of 2θ = 42.3° that could be due to Cu_2O (200) suggesting that both Cu^+ and Cu^{2+} species exist on this catalyst. Other features associated with CuO occur at Bragg angles of 58.3° (CuO(202)). There are additional peaks from CuO as well as two other peaks in the diffractogram for the evaporation-prepared Cu catalyst. All three peaks at Bragg angles of 2θ = 32.5°, 35.5° and 38.7° are due to CuO and have been identified by their respective Miller indices: (110), (-111) and (111). However, these three peaks are more intense than they appeared in the diffractogram for the filtration-prepared Cu catalyst and have narrower widths, indicating that evaporation has increased the degree of crystallization of CuO. A fourth peak occurs at a Bragg angle of 61.5° and has been assigned to CuO(-113), again showing evidence of better-defined copper-oxide phase formation. The peaks in the region of Bragg angles 42-43° remain indicative of Cu_2O (200).

The XRD pattern for the ZnO-based catalyst prepared by filtration clearly shows the reflections typical for a hexagonal structure of ZnO with reflection maxima located in 2θ angles of approximately 31.7°, 34.4°, 36.2°, 47.5°, 56.6° and 62.8°; they are related to ZnO (100), (002), (101), (102), (110), and (103) lattice planes, respectively. The maximum at 24.8° is due to the presence of halloysite. The evaporated Zn catalyst had the same ZnO peaks, but they had better intensity and peak resolution than before. Additionally, higher angle ZnO peaks (approximately 67.9° and 69.1°) corresponding to ZnO (112) and ZnO (201) could be seen more clearly. No other Zn containing phases were detected so this data shows that Zn is primarily in the form of ZnO. These results clearly demonstrate that evaporation promotes stronger crystallization and phase development of ZnO compared with filtration.

The XRD data for both the Ni catalyst prepared by filtration and the Ni catalyst prepared via evaporation show reflection peaks from the NiO(111), NiO(200) and NiO(220) lattice planes corresponding to 2θ = approximately 37.2°, 43.3° and 62.9° respectively. The presence of these three peak values confirms that cubic NiO is present as the major nickel containing compound within the catalysts. XRD spectra from the evaporation prepared Ni catalyst exhibit identical NiO(111), NiO(200), and NiO(220) lattice plane reflections. This demonstrates that the NiO phase composition has been preserved; however, the breadth of each peak value indicates that there may have been some degree of either particle size reduction or an improvement in the extent of dispersion of the NiO onto the support surface. There was no indication of any other nickel-containing compounds.

Overlapping reflections in the XRD pattern for the filtration-processed composite catalyst indicate the presence of multiple oxide phases. The peaks at 2θ = 31.7°, 34.4°, and 36.2° can be assigned as the (100), (002), and (101) planes of ZnO. The peak near 37.2° is due to NiO(111) and the broad area centered on approximately 43.3° could be due to NiO(200), or could also contain an overlapping contribution from Cu_2O(200). The broad area at 35-36° likely represents an overlapping combination of the (101) plane of ZnO, CuO(-111), and Mn_3O_4(211). Additional features near 47.5°,

 doi:10.20944/preprints202604.0621.v1

56.6-58.3°, and 62.8-62.9° are consistent with ZnO(102)/(110)/(103) and there appears to be some overlap from MnOx and NiO(220). XRD patterns from the evaporation processed composite indicated similar phase compositions but with slightly better definition of ZnO (100), (002), and (101) peaks. The peak corresponding to NiO(111) at 37.2° was still present and the broad peak area centered at approximately 35-36° continued to represent overlapping peaks from ZnO, CuO, and MnOx. This suggests that the high degree of integration of metal oxides continues after processing by evaporation. Evaporation redistributed the oxides so that they did not produce clearly defined crystalline phases.

The overall results of the XRD indicate that the preparation methods have different effects on the crystallization and distribution of oxides depending upon the metal used. For both zinc and copper, evaporation increased the crystalline of their respective oxides. Evaporation increased the intensity of the peaks for ZnO (100), ZnO (002), ZnO (101), CuO (110), CuO (-111), Cu_2O (111). For manganese and nickel, evaporation resulted in wider peaks indicating better dispersion of the manganese and nickel oxide phases. In addition, evaporation was found to improve phase definitions in the composite catalyst by reducing overlap but did not produce any significant separation of phases. Because there was peak overlap for many of the samples analyzed, primarily for the composite catalysts, some peaks were assigned to multiple possible oxide phases. Therefore, each peak is described in terms of its most probable assignment(s) as a primary contribution from one or more possible oxide phases.

2.1.3. FTIR Analysis of Catalysts Prepared by Filtration vs Evaporation

The FTIR spectra for the prepared catalysts (**Figure 2**) indicated a combination of vibrational characteristics of halloysite as well as other bands related to adsorbed species, surface hydroxyls, and deposited metal oxides on the surface. All catalysts exhibited significant absorption within the regions around 3600-3700 cm^{-1}, 3200-3500 cm^{-1}, 1630 cm^{-1}, 1000-1100 cm^{-1}, 910 cm^{-1} and less than 700 cm^{-1}. The broad absorption in the region 3600-3700 cm^{-1} can be attributed to stretching vibration of hydroxyl groups attached to the internal structure of halloysite as well as its inner surface. The broad absorption in the region 3200-3500 cm^{-1} can be attributed to hydrogen bonded OH stretching due to adsorbed water and surface hydroxyl groups. The absorption in the region 1630 cm^{-1} can be attributed to bending of molecularly adsorbed water. The intense absorption in the region 1000-1100 cm^{-1} is associated with Si-O stretching vibrations of the aluminosilicate framework. The absorption at 910 cm^{-1} has been associated with Al-OH deformation. Bands below 700 cm^{-1} have been shown to correspond to metal-oxygen lattice vibrations of the supported transition metal oxide species [10,24–27]. Both methods of preparation resulted in retention of bands corresponding to the fundamental framework; however, there was noticeable difference in the relative intensities, sharpness and visibility of each feature between filtration and evaporation preps. This indicates that the method used for preparing the sample affected both surface chemistry expressions and interactions between the metal and support.

 doi:10.20944/preprints202604.0621.v1

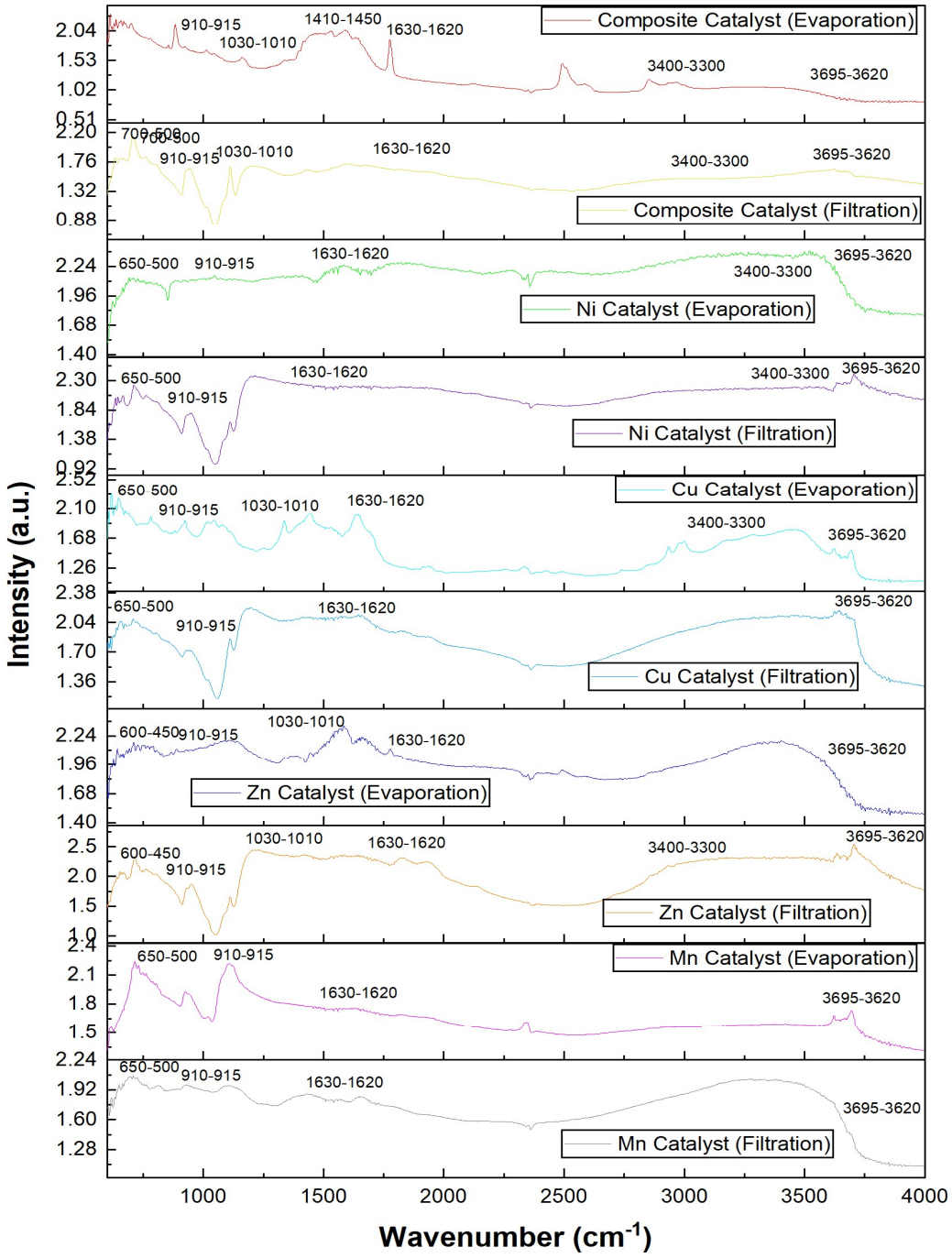

Figure 2. FTIR Spectrum of the Catalysts.

The evaporation-prepared composite catalyst had an organized FTIR structure than did its filtration-prepared analog. The FTIR spectrum of the evaporation-prepared composite catalyst indicated a somewhat broad hydroxyl envelope (3200-3500 cm^{-1}) in the higher wavenumber area. Within this region the hydroxyl envelope was centered roughly about 3380-3420 cm^{-1} and there was a reasonable water bending component apparent in the lower wavenumber area (1620-1640 cm^{-1}) [10,24].

 doi:10.20944/preprints202604.0621.v1

In comparison, these components were less pronounced in the FTIR spectra of the filtration-prepared composite catalyst; in fact, the higher wavenumber region of the latter appeared flat and less resolved. The presence of more intense O-H/H-O-H components in the FTIR spectra of the evaporation-prepared composite catalyst indicates either a larger number of available sites on the surface of the material to be functionalized (i.e., surface hydroxyl groups), or a more extensive development of the polar aspects of the surface of the particles. The evaporation route to prepare composite catalysts produced more distinct spectral peaks in both the lower wave-number region (framework related) and in the very low wavenumber region compared to those generated via filtration routes. There was evidence of a peak associated with the Si-O bond-stretching vibration (1020-1040 cm^{-1}) as well as a smaller, but still present, shoulder due to Al-OH deformation (910-915 cm^{-1}) in both samples. However, it was clear from visual inspection of these two figures that these bands were more defined and resolved in the case of the evaporation route. Similarly, more distinct absorption peaks were observed below 700 cm^{-1} in the spectra obtained using the evaporation route. The positions of these absorptions corresponded closely to values typically reported for vibrational modes involving oxygen-metal bonds in mixed oxides. In contrast, the lower wavenumber portion of the spectrum generated using the filtration route was smooth and much less resolved than that obtained using the evaporation route [6,26–28].

FTIR spectra from samples of the Ni catalyst prepared using either method exhibited variations as a function of preparation method. A weak broad absorption band was observed for the evaporation-prepared Ni catalyst located within the 3300-3450 cm^{-1} range and a corresponding band was found for the presence of adsorbed H_2O centered near 1625-1635 cm^{-1}. Bands corresponding to these functional groups were less defined for the filtration-prepared Ni catalyst and its FTIR spectrum appeared relatively flat throughout the same spectral region. The increased apparent intensity of OH/H_2O related bands present in the evaporation-prepared sample indicated that the nickel containing surface remained more readily available for reaction post synthesis and thermal treatment. Stronger metal/support interface interactions or more exposed oxide surfaces may have contributed to this [24,26]. The evaporation prepared Ni catalysts displayed improved resolution in the Si-O stretching band near 1030 cm^{-1} and Al-OH deformation band near 910 cm^{-1} compared to those prepared via filtration indicating that the structure of the halloysite support was maintained. Improved resolution was also noted in the low wavenumber 540-580 cm^{-1} where reasonable assignments could be made for Ni-containing metal-oxygen vibrations. Reduced responses were observed for the filtration-prepared samples. The observed trends are consistent with the idea that better retention of nickel bearing oxide species occurred at the outer or near-surface area of the support for preparations involving evaporation, whereas filtering resulted in reduced retention or weaker dispersions [6,13,27].

The zinc catalyst has some of the most notable distinctions based on how it is made; the evaporated Zn catalyst showed an apparent increase in the broadness of its O-H band within the 3360-3430 cm^{-1} range and an increased visibility of its band at 1625-1635 cm^{-1}. This indicates there is adsorbed water present as well as surface hydroxyl groups. The bands associated with hydroxyl groups were much less pronounced and clearly definable in the filtered Zn catalyst. This demonstrates that the evaporated Zn catalyst appears to have a more active surface chemistry and will be more effective at chemisorbing or adsorbing the sulfur containing molecules [10,24]. The same two Zn catalyst samples presented similar Si-O stretching bands (1030 cm^{-1}) and Al-OH deformation bands (910 cm^{-1}) in the fingerprint region. However, the evaporated Zn catalyst demonstrated a greater intensity of a band located within the 500-550 cm^{-1} wavenumber range. Bands within this wavenumber range are typical of metal-oxygen bonding in zinc-containing oxides. Conversely, the filtered Zn catalyst showed a less defined and flatter response in the same area. In addition, the filtered Zn catalyst had a smaller shoulder in the 1400-1450 cm^{-1} wavenumber region compared to the evaporated Zn catalyst. It would appear reasonable that this could be due to either remaining acetate/carbonate type surface species, common in many oxide-based catalysts that use acetates as their precursor. Overall, these data suggest that the evaporative process produces a Zn-containing

 doi:10.20944/preprints202604.0621.v1

oxide surface with functional groups while the filtering process produces a weaker surface that expresses fewer chemical properties [6,29].

Although the Cu-catalyst followed the same pattern as shown for Al_2O_3, this Cu-catalyst seemed to follow a more extreme trend. Bands for both the hydroxyl and fingerprint regions could be seen in better detail in the Cu-catalyst prepared through evaporation compared to its counterpart prepared using filtration. More defined bands were observed at 3380-3440 cm^{-1} and a much less intense band around 1630 cm^{-1} in the evaporation samples, these can indicate that there are a greater number of surface hydroxyl groups present (or that water is being held to some extent) to an active site. Conversely, the filtration-prepared Cu catalyst demonstrated a flat, poorly resolved high-frequency region, implying that it had fewer chemical sites exposed [10,25]. In addition, the Cu-catalyst prepared via evaporation demonstrated more pronounced support responses in the vicinity of 1030 cm^{-1} and 910 cm^{-1} and appeared to have a more distinct lower frequency absorption in the range of 570-620 cm^{-1}. These observations would logically result from Cu-containing metal-oxygen vibrations. Although filtration-prepared Cu-catalysts retained most of the same general support related bands they demonstrated less intensity and less resolution in their lower frequency profiles. As such, it appears that the copper containing oxides were better retained (and/or more strongly expressed) at the surface when evaporation was utilized. It is consistent with what is expected due to filtration, i.e., dissolution/weak association of portions of the Cu precursor species will be removed from solution during filtration prior to calcination [6,26,28].

There are notable FTIR differences (in terms of Mn) between different methods use to prepare the Mn catalyst. The Mn catalyst prepared by evaporation had an absorption peak at a higher wavenumber (3300-3450 cm^{-1}) compared to the absorption peak for the filtration-prepared Mn catalyst; and there was a visible peak (1630 cm^{-1}) in the case of the Mn catalyst prepared by evaporation. These peaks are consistent with the presence of several surface-exposed hydroxyl groups associated with water on the catalyst. This contrasts sharply with the Mn catalyst prepared by filtration, where the absorption peaks in the higher wavenumber region were significantly less apparent and those in the mid-wavenumber region were reduced. It is reasonable to conclude that the method of preparing the Mn catalyst has influenced the degree to which the Mn-containing surface environment remains chemically available [10,24]. There were similar bands in both Mn catalyst samples related to the halloysite-based support in the lower wavenumber region. However, there were more pronounced bands in the lower wavenumber region (< 700 cm^{-1}) for the Mn catalyst prepared by evaporation than for the filtration-prepared sample, especially in the range of 540-590 cm^{-1}. These bands are typically indicative of metal-oxygen bond vibrations involving manganese. These bands were weaker and less well-defined for the filtration-prepared Mn catalyst. These results indicate that there are differences in the manifestation of manganese bearing oxide species on these surfaces, as well as in the extent of interaction between the metal and support phases. The absorption spectrum from the evaporation sample appears to be more defined than that from the filtration-prepared sample; therefore, there are differences in the retained surface expression of the active oxide phase on these two surfaces [6,26,27].

Generally, when we compare the exact same metal (the catalytic material) for both evaporation prepared catalysts and filtration prepared catalysts, there is an overall FTIR trend: evaporation prepared catalysts have typically demonstrated stronger and more easily identifiable bands related to their surfaces as opposed to the filtration prepared counterparts. The above trend was shown through all three regions of interest; specifically: the hydroxyl/ water band (3200-3500 cm^{-1} and 1630 cm^{-1}); the halloysite frame work band (1030 cm^{-1} and 910 cm^{-1}); and particularly in the low wavenumber region under 700 cm^{-1}, where metal-oxygen vibrations could be distinguished in the evaporation-prepared samples, but not so much in the filtration-prepared samples. This pattern indicates, scientifically speaking, that the evaporation process favors retention on the surface and thus better exposure of the deposited metal precursor species, ultimately resulting in a catalyst surface exhibiting greater FTIR spectral representation of hydroxylated sites and metal-oxygen functionality. Conversely, filtration likely resulted in removal or distribution of some degree of

 doi:10.20944/preprints202604.0621.v1

soluble or weakly bound precursor species during processing, resulting in less intense and less distinct FTIR bands associated with metals. As such, although FTIR cannot measure the amount of metal present in a sample, the spectra do demonstrate qualitatively that the catalysts generated via evaporation processes exhibit higher degrees of chemical expressiveness and surface accessibility of active functionalities relative to those generated via filtration, as evidenced by the observed differences in catalyst performance and as supported by the results obtained using the other analytical methods used to characterize these materials [6,26,28,29].

2.1.4. EDS Analysis of Catalysts Prepared by Filtration vs Evaporation

The EDS data proved the existence of both the anticipated support-derived and metal-derived species within the prepared catalysts and demonstrated that the method of preparation had a significant influence on both the amount of surface elemental retention as well as elemental accessibility as shown in **Figure 3**. As would be expected due to their composition, Al, Si and O peaks were consistent across all of the samples as halloysite has been previously reported to have a chemical distinction between its outer surface layer rich in silica and the inner surface layer rich in alumina [10,30,31]. Additionally, each of the respective catalysts exhibited the signal of the appropriate active metal peak as either Mn, Cu, Zn or Ni. However, it was noted that the composite catalysts simultaneously presented multiple signals from different transition metals as expected. However, the relative size of the metal peaks varied significantly between those catalysts made via filtration versus evaporation methods, suggesting that the method used for making the catalyst impacted how much of the metal-phase that had been deposited onto the catalyst existed at the catalyst's surface post-synthesis and calcination.

 doi:10.20944/preprints202604.0621.v1

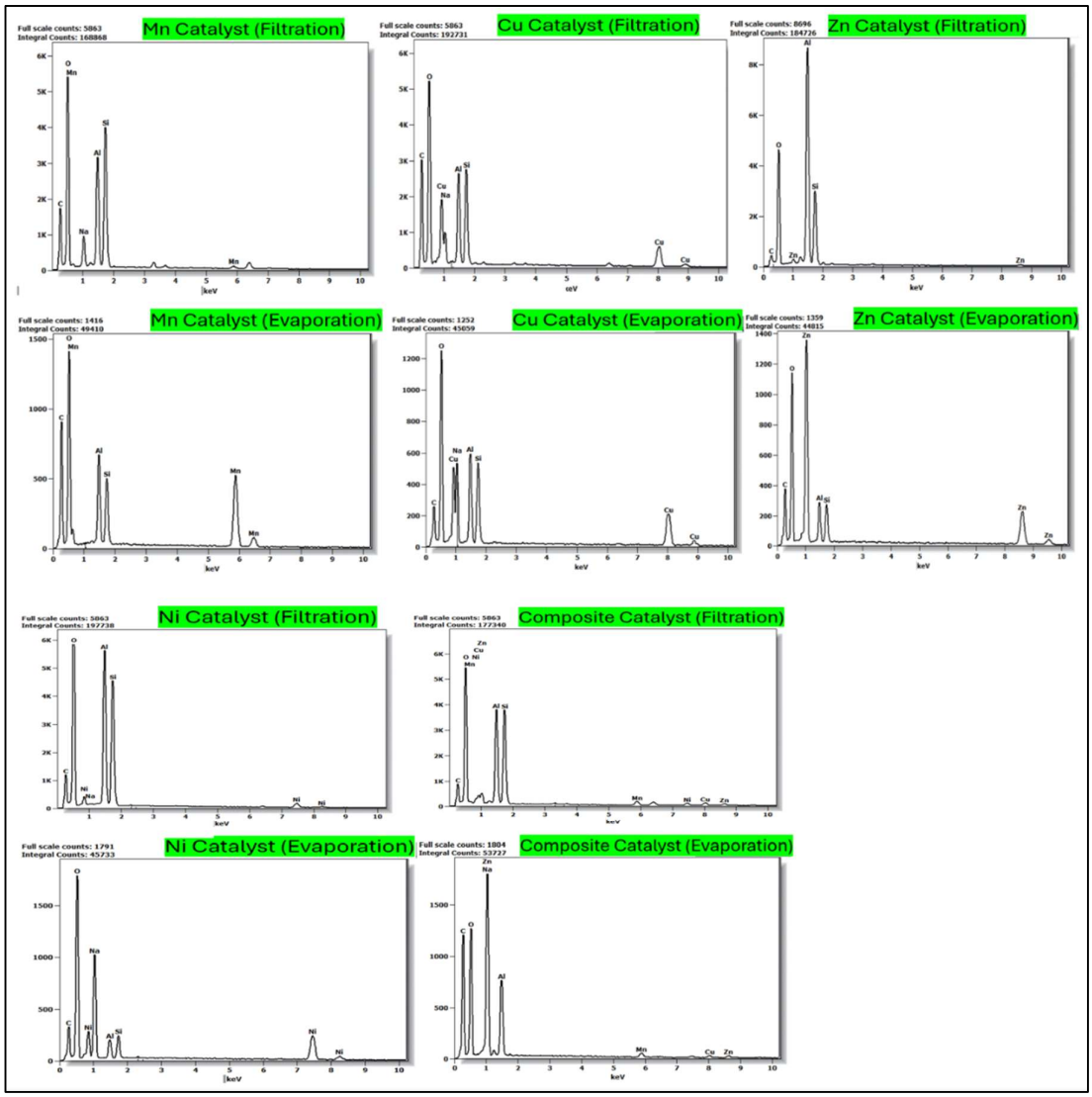

Figure 3. EDS Spectrum of the Catalysts.

The preparation of the manganese catalyst exhibited an evident dependence on the element distribution. A considerable presence of Na, O, Al and Si was evident within the EDS data for the filtration prepared Mn catalyst which corresponded well to each of these respective elements and demonstrated additional peaks for Mn. The presence of both Al and Si was reasonable due to their identification as support material elements. The presence of both Al and Si suggests that some portions of the analyzed surface area had been retained in a manner consistent with halloysite-based support rather than having been uniformly coated by Mn-containing moieties. Sodium could be present due to the use of sodium hydroxide during the pH adjustment step, and it has previously been shown that sodium-containing species may remain in supported oxides that have been prepared from alkali containing media [13,32]. By comparison, the EDS spectra showed that the evaporation-pretreated Mn catalyst had a higher proportion of Mn-signal at the surface compared to the other signals from the support. In particular, the EDS spectra indicated a greater intensity of both low energy signals and the characteristic Mn-signal for the evaporation pretreated sample when compared to the other sample. The presence of Al and Si were still evident as they are part of the halloysite but, their intensities were less prominent than those observed with the filtered sample. These results indicate that there was an increased enrichment of Mn-species at the surface of the

 doi:10.20944/preprints202604.0621.v1

halloysite following evaporation treatment. The significant difference observed indicates that the use of evaporation was able to retain a larger portion of the manganese precursor on the halloysite surface before calcination, leading to a greater number of Mn-oxide species being exposed on the surface. From a scientific point of view, it is highly relevant to know whether the metal component is located at the accessible surface versus simply synthesized into the structure [6,33] since the adsorption and catalysis properties of transition-metal oxides depend heavily upon this factor. Thus, the data presented here supports that using evaporation enhanced Mn-surface retention for the Mn-catalyst when compared to using filtration.

The filtered copper catalyst had an EDS spectrum which displayed clearly defined peaks for Cu as well as O, Al, Si, and Na. However, the presence of significant framework-related expression from the Al and Si peaks indicated that the support was very largely unobscured (i.e., very largely exposed) to the probe. Therefore, while there is evidence that Cu was present on the catalyst surface, it appears that this surface was substantially composed of exposed support rather than being dominated uniformly by Cu containing oxides. In comparison, the evaporated Cu catalyst presented an increased total expression of copper containing surface species as compared to the Cu present on the filter-derived surface. The Cu peaks are much more pronounced as compared to the peak intensity from the support material, which presents a more diminished presence for both Al and Si as well when compared to the filtered sample. Therefore, it appears that the majority of the copper precursor remained during evaporation and then underwent conversion into Cu-containing oxides on the surface of the catalyst. Copper-based precursors may remain somewhat soluble in their mother liquor throughout the synthesis process. As such, some portions of these copper-containing species may be removed by filtration prior to achieving full coverage and subsequent deposition onto the solid-state [8,9,21].

The nickel catalyst exhibited similar contrasts to those seen for the filtration prepared Ni catalyst. The EDS of the Ni containing species on the halloysite support revealed Ni along with O, Al, Si, and Na. However, the EDS remained heavily influenced by the peaks from the support itself, particularly in the Al-Si regions. Thus, there is evidence that the framework of halloysite has significant exposure at the surface. As such, it can be inferred that while nickel may exist as species within the halloysite framework, the nickel surface abundance or dispersion may be limited by the method used to filter the catalyst. The Ni peak in the Ni catalyst with evaporated Ni is stronger compared to its support peaks than those of the framework-derived Al and Si peaks. The strength of the Ni peak versus the support peaks suggests that there is better preservation of the Ni-containing species on the available surface area after using evaporation. Wet processing is known to cause significant redistribution of nickel containing compounds as soluble salts. When drying or calcining occurs, if all of the nickel salt has not been immobilized before removal from the solution, then it will be difficult to obtain high surface concentrations of the nickel component after drying/calcining [6,8].

The multi-metal composite catalyst had the strongest evidence for demonstrating the influence of a specific preparation technique on its performance. With the multi-metal composite being prepared by filtration, the EDS analysis revealed the expected presence of Zn, Cu, Mn and Ni along with O, Al, and Si (from the carrier). The EDS analysis remained heavily dominated by the carrier with both Al and Si continuing to show high intensity. Thus, although there was evidence for the presence of each of the intended active metal oxides in the composite, they did not appear to be as richly surface enriched as desired. In comparison, the distribution of the metallic active sites was much more apparent on the surface of the evaporation-prepared composite catalyst than the distribution on the filtration prepared catalyst. The transition metal peaks from both metals are very evident in relation to the peaks representing the halloysite support material. Although Al and Si would be expected in this case due to it being a supported catalyst, the surface appears less influenced by the support structure and appears to be representative of the desired active mixed-oxide composition. This observation is important as multi-metal oxide-based catalysts do not solely depend on having each metal present individually on the surface, they require the metals to be deposited in such a way as to allow them to remain together as an accessible surface entity post-synthesis [33,34].

 doi:10.20944/preprints202604.0621.v1

Comparing the two samples using EDS, we found the Zn-catalyst to be one of the best comparison cases available within the data set. The filtration prepared-Zn catalyst EDS showed the expected Zn signal along with significant support related signals from O, Al, and Si. However, the filtered Zn sample also had extremely high intensities of both Al and Si, suggesting that while Zn was effectively introduced into the system, the filtered sample did not produce the level of surface area saturation or surface enrichment by Zn containing species which would have been seen if it were prepared using a more retention efficient method. The comparative analysis indicated an increased presence of Zn relative to the peak intensities of Al and Si within the halloysite-based framework. A significantly higher intensity and surface-dominance of Zn-containing peaks compared with Al- and Si-peaks indicated that the evaporation methodology resulted in better retention of the zinc-containing oxides at the surface of the material. A larger metal-to-support ratio of signals from X-ray microanalysis typically indicates that the active phase has a higher degree of surface accessibility in supported metal oxides. Provided the support does not change, and the measurement parameters are kept constant [32,33] this suggests that a large metal-to-support ratio supports the assumption that the retention by evaporation was better than the filtration method.

In comparison, the distribution of the metallic active sites was much more apparent on the surface of the evaporation-prepared composite catalyst than the distribution on the filtration prepared catalyst. The peaks from the metals are evident in relation to the peaks representing the halloysite support material. Although Al and Si would be expected in this case due to it being a supported catalyst, the surface appears less influenced by the support structure and appears to be representative of the desired active mixed-oxide composition.

2.1.4. SEM Analysis of Catalysts Prepared by Filtration vs Evaporation

SEM (scanning electron microscopy) imaging was used to compare the surface structure and topography of the catalyst's samples prepared using both evaporation and filtration (see **Figure 4**), although each sample had an identical composition. The primary distinctions among the preparations lay in their respective particle textures, surface smoothness/roughness, degree of aggregation, and porosity. The results indicate that the method employed for removing solvents from catalyst solutions prior to calcination has a profound influence on the ultimate morphology of supported metal oxides. Filtration preparations produced relatively smooth, dense, and uniform surfaces, while evaporation preparations resulted in significantly rougher, more fractured, and more porous morphologies. These observations are consistent with theoretical understanding of catalyst preparation procedures, which indicate that evaporation facilitates the distribution and precipitation of metal precursors into the pores of the supporting material, while filtration may result in some loss or non-uniform depositing of catalytic [6,8,28].

 doi:10.20944/preprints202604.0621.v1

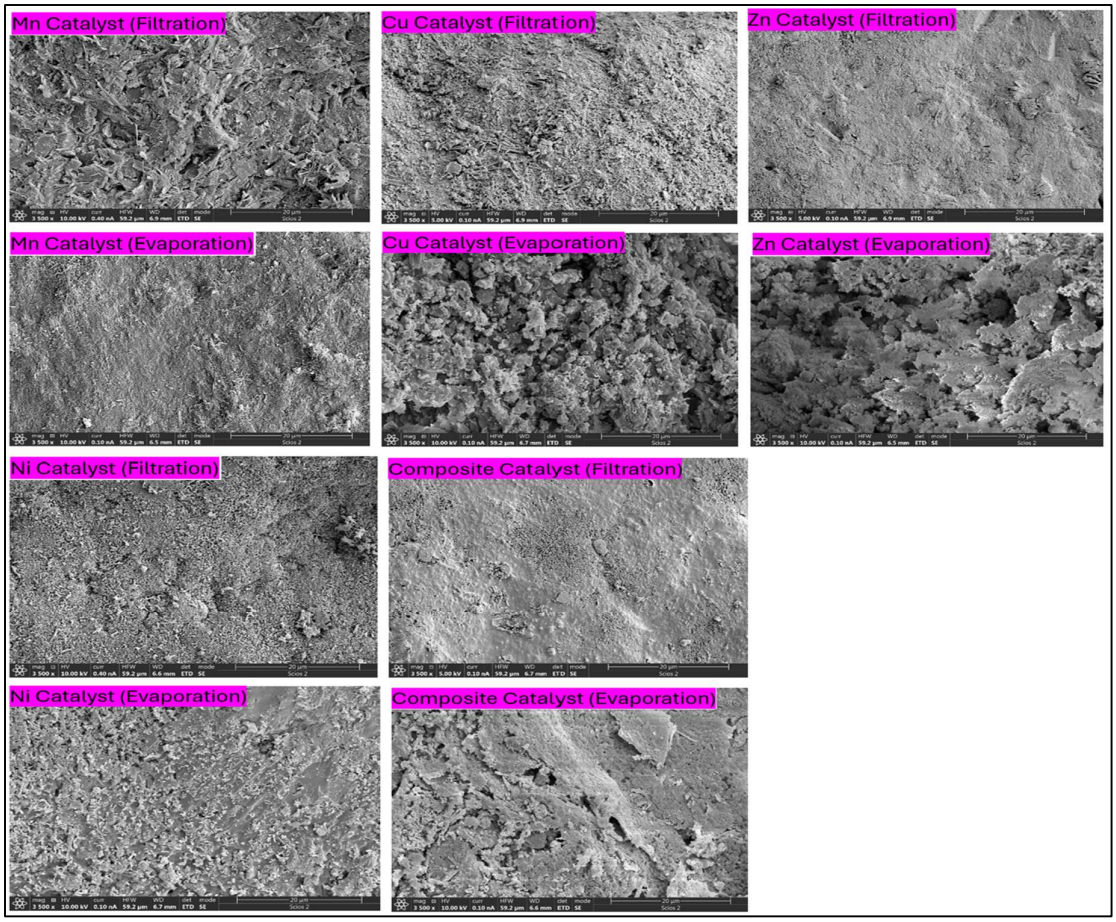

Figure 4. SEM of the Catalysts.

The Mn catalyst synthesized using filtration demonstrated a relatively flat and layered structure with primarily plate-like morphological features, along with very little visual evidence of pores. The surface also presented an aggregate appearance as well as slightly flattened with areas of particle overlap in addition to a lack of observable open pore channels. These characteristics suggest that most of the precursor solutions may have been filtered out before uniform deposition occurred resulting in a structure predominantly formed from the supporting substrate with minimal redistribution of manganese species. Unlike the Mn catalysts prepared through evaporation the Mn catalyst formed using evaporation presented a distinctly unique morphological appearance due to its homogenously rougher texture containing much more extensive structural irregularities. The appearance of these particles indicated they were smaller in size, more loosely arranged, using evaporation and contained observable microscopic structure related to an increase in particle fragmenting. These characteristics indicate the evaporation technique provided the opportunity for manganese-based precursors to be maintained in solution until such time as the solvents were slowly being removed at which time it would have been deposited onto the substrate in a relatively uniform manner. The behavior described above is typical of the development of more uniformly dispersed oxides and improved metal/support interactions. It has been reported that improvements in the uniform dispersion of oxides and interactions between metals and supports can improve both the surface accessibility and catalytic efficiency of supported catalysts [32,33].

The morphology of the Cu-catalyst synthesized using filtration demonstrated a relatively uniform and dense surface. The Cu-surface exhibited little to no variability in terms of particle size and limited porosity was visually observed on the surface. However, the Cu-surface did exhibit an aggregated domain that may be indicative of particles being coalesced during the calcination process.

 doi:10.20944/preprints202604.0621.v1

Such structures are typically related to reduced accessibility to active sites due to pore collapse or pore development limitation resulting from a lack of precursor distribution [18,19]. The structure of the copper catalyst made by evaporating the solution had much more porosity in it and many different shapes to it than the other. It also had large clumps of particles that were stuck together and the clumps had many pores in them. This indicated that there would be a greater number of pores in this catalyst due to the way the solvent was removed as well as how well the Cu containing species were dispersed throughout the support. Catalysts of these types generally have a larger surface area and better access to the reactive sites on their surface. Therefore, they are generally good at adsorbing molecules [6,33].

The filtered Zn catalyst had an essentially unblemished and very flat (relatively) surface compared to that of other materials, with little evidence for porosity or surface irregularity, which is indicative of the compactness of this morphology. There were a few small surface defects present but overall, the surface was quite even. It appears as if filtration led to a structural predominance of support material relative to that of the zinc-containing species on the surface. Further it can be inferred that there is little particulate evidence on the surface of this Zn catalyst, which could indicate that the deposition of Zn precursors was either non-uniform or some of these were removed by filtration. In contrast to the Zn catalyst produced through evaporation was found to be very porous and textured in nature as well as have an irregular shape consisting of many loose clusters. It has been shown through the presence of large irregularly shaped cluster groups along with empty space within these groups that there are better distribution and deposition of the Zn containing material on the support. These features are indicative of larger surface areas and greater numbers of available reaction sites which are essential for the adsorption of Sulfur onto Zn based catalysts [35,36]. Therefore, it can be concluded that the evaporation method results in structural improvements over filtration method for Zn based catalysts.

The surface of the Ni catalyst produced through filtration was very uniform and well-distributed; there were numerous small particles that exhibited high packing densities and low morphological variations throughout. The surface of this catalyst appeared to be mostly smooth with some minor roughness and few visible pores. These results suggest that the filtration process had yielded a morphology where the support framework still dominated the surface while possibly minimizing the exposure of Ni-containing catalytic sites. In contrast to the morphology obtained in the case of the morphology of the evaporated nickel catalyst was significantly more disordered and fractured. This is due to an increase in the amount of surface roughness that can be observed and by the formation of loose clusters or agglomerates of particles. The characteristics suggest both increased porosity within this material and a greater degree of dispersion of nickel. These characteristics are consistent with the occurrence of significant metal-support interactions that enhance access to active sites necessary for catalysis and/or adsorption [8,28].

The composite catalyst prepared through filtration showed a relatively flat, smooth and consistent surface area. There was a significant amount of continuity to this surface area; there were very few texture changes to this surface. Porousness could also be observed on the surface. However, since the morphological characteristics of this surface were solidified; it can be inferred that all metal precursors are not being equally distributed throughout synthesis. Unlike the composite catalyst made through evaporation, the composite catalyst formed by evaporation has a very diverse and open structure of pores as well as an extremely rough surface. It can be seen in micrographs that this sample contains large agglomerates of particles. The fact that there are large groups of irregularly shaped particles, which appear to be loosely connected by voids, indicates that the metal precursors from each component were kept intact and deposited together upon evaporation. Morphology of composite catalysts is especially significant for multicomponent mixed metal oxides. For these types of materials, the catalytically active sites must be close enough, so they interact when reacting with reactants. As such, the increased structural diversity observed in the composite catalyst produced by evaporation may result in both greater access to surface sites and possible synergy between the individual metal components [33,34].

 doi:10.20944/preprints202604.0621.v1

The morphology of each catalyst pair was examined, all pairs exhibited two distinct trends: The filtration prepared samples showed a smooth, dense structure with little heterogeneity in terms of surface topography. Samples prepared using evaporation demonstrated a much rougher, highly porous, and very heterogeneous surface morphology. The differing morphology for each preparation method may be due to how the solvent is removed from the sample. Evaporative methods allow the solvent to be slowly removed, allowing the solute to precipitate in-situ as it is being deposited onto the support material. This process allows for greater dispersal of the solute and potentially greater pore development. Filtration methods remove the liquid phase before all of the solutes have been deposited on the support. Since this method does not allow time for all solute particles to deposit onto the support, some solute may be lost during the filtration process or may fail to achieve full surface coverage [6,28]. The SEM analysis shows structural differences between the two methods, and it indicates that structural optimization can be achieved through better morphology. The structural changes caused by evaporation will likely increase surface area, improve diffusion properties, and make the reaction sites available for the reactants. This makes evaporation an advantage over filtration. Rougher surfaces, high porosity and dispersed particles all enhance diffusion rates and access to reactive sites.

2.1.5. XPS Analysis of Catalysts Prepared by Filtration vs Evaporation

The XPS spectra provides valuable insight into the impact of the solvent removal on both the location of the metal species and the extent of the outer surface area of the halloysite as shown in **Figure 5**. As an example of this, the presence or absence of significant halloysite-related peaks such as O 1s, Si 2p, and Al 2p would be indicative of how much of the halloysite has been exposed. Conversely, the presence of carbon C 1s, typically used as a reference point for charging effects, would indicate that the surface had some amount of adventitious carbon present. All these data collectively indicate that there is considerable variation in the distribution of active metals depending upon whether they have been removed by evaporation or filtration. Additionally, it appears that the evaporation route tends to produce a greater degree of metal retention on the surface compared to filtration in many of these samples. This indicates either improved metal retention during calcination and/or better metal deposition onto the surface. For assigning the peak locations associated with the halloysite support, the reported positions in the literature for other aluminosilicate materials like halloysite are in good agreement. Also, since all the transition-metal core-level position assignments agree well with those expected for their respective metal-oxide states post-calcination [10,37].

 doi:10.20944/preprints202604.0621.v1

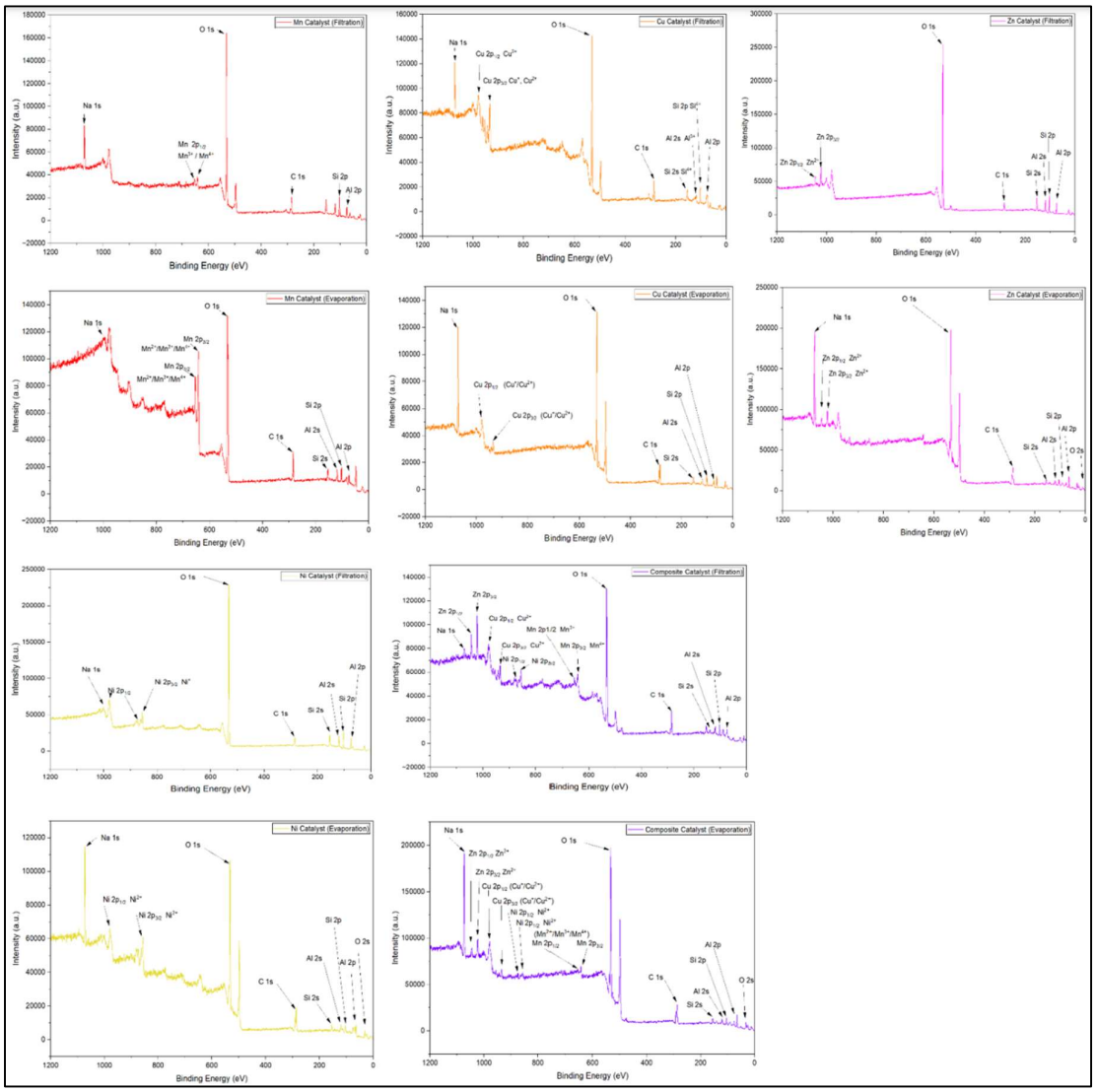

Figure 5. XPS Spectrum of the Catalysts.

The XPS spectra of the manganese catalytic systems has shown that all materials contained Mn, O, Si, Al and C, which shows that there is an important distinction between the two preparation methods. The filtration method produced a Mn 2p spectrum for the Mn catalyst that had a very weak and broad Mn 2p signal. It can be seen from this spectrum that while Mn was present on the surface of the material, it made up only a small fraction of the signal relative to that of the support. Mn 2p peaks were located at 641-643 eV (Mn $2p_{3/2}$) and 653-655 eV (Mn $2p_{1/2}$). These values corresponded to manganese in the form of primarily mixed Mn^{2+}/Mn^{3+} oxide species, rather than metallic Mn. The peak at 531-533 eV corresponding to O 1s also indicates that the manganese was present as an oxide. The Si 2p and Al 2p peaks were both clearly evident, indicating a significant portion of the outer surface of the halloysite clay support was exposed. This indicates that during the filtration process some of the manganese precursors were less efficiently retained to the support surface or did not distribute evenly throughout the available outer regions of the catalyst [38,39]. In contrast, the Mn catalyst prepared using evaporation showed a much clearer and more defined Mn surface profile than filtration. Specifically, the Mn 2p peak was seen as being above the background support level more so than the filtration prepared Mn sample. As such, while there appeared to be no significant difference in terms of the Mn oxidation state (i.e., Mn^{2+}/Mn^{3+}), the fact that there appears to have been significantly more surface-bound Mn species present on the evaporation prepared Mn catalyst would suggest that this preparation method retains more manganese species in proximity to the surface of

 doi:10.20944/preprints202604.0621.v1

the catalyst. The lower presence of the support peaks relative to those associated with the Mn species is also consistent with a higher degree of surface area coverage by Mn-oxide species. Surface enrichment of these Mn-oxide species should be more conducive to direct sulfur adsorption onto the Mn-oxide species along with redox assisted interactions with sulfur compounds (example ethyl-mercaptan). Thus, based on the XPS data presented here, it appears that evaporation provides better preservation of the surface Mn-oxide species compared to filtration.

The XPS spectra of the Cu-catalysts indicates the presence of Cu, O, Si, Al and C; however, there were significant variations observed in terms of the relative intensities of the Cu-surface signal among the two different synthesis methods. The Cu 2p-region for the Cu catalyst prepared by filtration, was identified to be near 933-935 eV (Cu $2p_{3/2}$) and 953-955 eV (Cu $2p_{1/2}$) which are indicative of an oxidized state of Cu. When examined at a general survey level, it can be concluded that these peaks arise from Cu^{+} /Cu^{2+} oxides; this conclusion is made since Cu_2O-like (Cu^{+}) and CuO-like (Cu^{2+}) are typically distinguishable using high resolution Cu 2p analysis and ideal satellite evaluation. Therefore, when a large O 1s peak is present in conjunction with the Cu-peaks, this supports the claim that copper is in an oxidized form as opposed to being metallic. In comparison, the evaporated Cu catalyst showed an even clearer Cu 2p signal than before, with a higher Cu-related intensity compared to the halloysite background. Thus, it can be concluded that the method of evaporation resulted in a greater portion of Cu being deposited on the exterior surface or promoting better formation of Cu oxides over the entire support. Furthermore, since surface copper-oxide states have a strong interaction with sulfur containing adsorbents, the greater Cu-signal at the surface is structural. Additionally, since there was no indication of metallic Cu in the spectrum and the Cu 2p-binding energies remained consistent with the oxidation state of copper (Cu^{+}/Cu^{2+}) as expected after calcination of the precursors, it appears that the process effectively formed an oxide-based Cu-catalyst. Typically, in X-ray Photoelectron Spectroscopy (XPS), Cu^{2+} is identified by shake-up satellites located above the binding energy of the main peak in the high-resolution Cu 2p spectrum. Since shake-up satellites cannot be used to separate Cu^{+} and Cu^{0} definitively from the data alone, the most reasonable conclusion based on the spectra is that evaporation provided a greater amount of surface oxidized copper species than did filtration method, which correlates with the improved metal retention [37,40,41].

The XPS spectra of the zinc catalysts exhibited one of the most clear-cut and easily interpreted variations in comparison to how they were prepared. On the filtration-prepared Zn catalyst, the Zn 2p doublet showed up at about 1021-1023 eV (Zn $2p_{3/2}$) and about 1044-1046 eV (Zn $2p_{1/2}$). These energies for the Zn 2p doublet are indicative of Zn^{2+} species; these species are generally associated with ZnO type surface environments. The Zn 2p peaks were evident and thus indicated that a significant amount of zinc oxide had been deposited onto the halloysite support. However, due to the fact that the Si 2p and Al 2p signals from the support surface were relatively prominent, it appears that a considerable portion of the support surface remained largely unencumbered by the Zn oxide layer, indicating that while there was some degree of coverage by the Zn oxide layer, this layer was not maximally surface enriched. The XPS spectra of the evaporation-prepared Zn catalyst also displayed an even larger and clearer Zn 2p peak compared to those of the filtered Zn catalyst, indicative of a higher surface density of zinc species. The higher Zn 2p signal intensity seen for the evaporation prepared sample indicates that gradual removal of solvents by evaporation allowed a significantly larger amount of the zinc precursor to be retained in association with the support as it was dried and calcined, resulting in a larger fraction of a more Zn rich outer surface. The Zn 2p peaks were entirely consistent with Zn^{2+}; likewise, no evidence of metallic Zn was anticipated. For all Zn containing materials in XPS, Zn 2p binding energies around 1021-1022 eV are known to represent ZnO and related Zn^{2+} environments. As such, given the unambiguous nature of the oxidation states in these environments, especially compared to Cu or Mn, the XPS data for the Zn catalyst supports the premise that evaporation resulted in an increased surface retention/exposure of Zn^{2+} oxide species vs. filtration [37,38].

 doi:10.20944/preprints202604.0621.v1

The XPS spectra of nickel catalysts prepared using both methods showed peaks for all elements that are present in the samples including: Ni, O, Si, Al, and C. For the filtration-prepared Ni catalysts, peaks were observed at approximately 854-856 eV (Ni $2p_{3/2}$) and 872-874 eV (Ni $2p_{1/2}$) that correspond to a Ni^{2+} species such as NiO like environments. Furthermore, an O 1s peak was also observed which confirms the oxide nature of the nickel phase. Similarly to the filtration prepared Mn and Cu samples, support-derived Si and Al peaks remain relatively prominent indicating that the outer surface was not fully dominated by nickel oxide species. The Ni 2p from the evaporation prepared Ni catalyst has a much more obvious Ni 2p spectrum above the background noise from the support than does the filtration prepared sample. Thus, it appears that evaporation produced somewhat better retention of Ni containing surface species than did filtration. However, there was not an extreme increase in the amount of Ni at the catalyst's surface compared to the increases seen with either Zn or Cu. Despite this however, this trend still shows that evaporation provided a better means of retaining nickel containing species on the catalyst's surface. This is important from a structural standpoint since removal of sulfur by Ni is highly dependent upon having available Ni-O surface sites as opposed to having bulk amounts of nickel trapped within the support. Spectra of Ni 2p for NiO contain complex multiple structures and satellite peaks resulting from shakeup transitions, thus typically require high resolution XPS measurements to distinguish oxidation states beyond Ni^{2+}. As such the best possible interpretation is that evaporation resulted in preserving a slightly higher intensity of surface Ni^{2+} oxides than did filtration [37,42].

The spectra from the XPS study provided strong evidence at a surface level regarding how the method of preparation affected the overall multi-metal composition. For the filtration prepared composite catalyst, the spectrum indicated the simultaneous presence of Zn, Cu, Ni, Mn, O, Si, Al and C. This confirmed that all the desired metal components had been successfully incorporated into the material. Additionally, the Zn 2p doublet appeared as expected in the range 1022-1045 eV (consistent with Zn^{2+}); The Cu 2p doublet ranged as expected 933-935 and 953-955 eV (consistent with Cu^{+}/Cu^{2+} oxides). The Ni 2p doublets ranged as expected 855 and 873 eV (attributed to Ni^{2+}); And the Mn 2p doublets ranged as expected 641-643 and 653-655 eV (consistent with $Mn^{2+}/Mn^{3+}/ Mn^{4+}$ oxide). Although there is indication of all four metals present in the data, the support peaks remain very dominant which indicates that the filtration route may have produced some degree of multi-metal oxide but did not achieve high enough levels of surface enrichment. A comparison of the composite metal-oxide systems produced by evaporation and filtration indicated that while both systems exhibited the expected metal derived peaks, the peak intensity was significantly higher in the case of the evaporation prepared sample. Also evident from this data was a much-improved balance of transition metal features throughout the spectra region. These findings are consistent with evaporation providing a better means to retain the multi-metal oxide system as well as exposing more of the surface. In particular, the composite system prepared by evaporation was found to have a more uniform distribution of Zn^{2+}, Cu^{+}/Cu^{2+}, Ni^{2+}, and Mn^{2+}/Mn^{3+} species across its surface relative to the filtered system. This finding is very important because the effectiveness of the composite material will be directly related to the simultaneous availability of multiple active surface oxides. Therefore, based on these findings alone, there can be little doubt that evaporation provided superior preservation of the surface chemistry of the mixed metal oxide system versus filtration.

When combined, the XPS results show that the preparation route affected the surface chemistry of the catalysts to a large degree, although the nominal precursor chemistry was identical. Overall, across both the monometallic and bimetallic systems, the evaporation method typically gave rise to greater metal derived signal strengths which indicated that the active metal oxide species had been better preserved and exposed to the surface. The greatest evidence of this trend occurred with Zn and Cu; however, it is also apparent with Mn, Ni and the bimetallic sample. After calcination, all of the metals remained primarily as oxides (Zn^{2+}; Ni^{2+}; Cu^{+}/Cu^{2+}; Mn^{2+}/Mn^{3+}) whereas the presence of halloysite was still detected by Si and Al signals. These results have significant implications for catalytic sulfur removal as it is an inherently surface-based reaction; thus, the quantity and availability of the metal oxide species at the exterior surface will be much greater determinants to

 doi:10.20944/preprints202604.0621.v1

how well the catalyst works rather than simply being determined by how much metal is present within the catalyst. Therefore, the XPS data provide direct surface-specific proof that evaporation is a better method for preparing a catalyst when compared to filtration for maintaining active metal species on the surface of the catalyst, thereby supporting the enhanced structural integrity and adsorption properties observed throughout this investigation.

2.2. The Analysis of Catalysts Adsorption Performance

The adsorption of sulfur by catalysts made through both filtration and evaporation were studied using breakthrough tests at a 10ppm sulfur content (the breakpoint) as shown in Figure 8. The breakthrough curve indicated the preparation process greatly affected the performance of the catalysts, regardless of the catalyst's composition. All catalysts (evaporation method) exhibited a greater delay in sulfur breakpoint than those prepared via filtration. Therefore, it can be concluded that the route used to remove the solvent from the catalyst strongly influences the final effectiveness and accessibility of the active surface of the catalyst. The observed trend is consistent with theories for preparing supported catalysts, which indicate that the methods employed for drying and removing solvents can influence the redistribution of precursors during calcination, oxide formation, metal retention, and the ultimate surface accessibility [7–9,21]. The improvement in adsorption behavior of the catalysts produced through evaporation is due to the synergistic effects from various parameters as shown from characterization studies. EDS analysis suggested an enhanced retention of active metals on the catalyst prepared through evaporation. It is believed that evaporation resulted in lower loss of dissolved precursors during removal of the solvent (solvent evaporated) relative to physical separation of the solvent. Also, XPS confirmed that the surface metal signals of the catalyst prepared through evaporation were stronger; thus, it is believed that a larger fraction of the catalytically active phase remained available at the outermost surface. The results of XRD supported similar conclusions about the development of oxide phases and dispersion of these phases within the evaporation-produced materials. Additionally, SEM showed more fracturing, porosity, and surface roughness in the morphology of particles of the evaporation-prepared catalysts, whereas filtration-prepared catalysts had smoother and more dense particle morphology. Similarly, BET surface areas of both types of catalysts exhibited different levels of porosity and surface roughness. However, the results of this study suggest that neither the type of porosity nor total geometric surface area alone influenced the adsorptive performance of these two types of catalysts. Rather, it appears that accessible pore architecture combined with exposed surface metal oxides and retained chemically useful metal species are much more important for achieving good adsorption than is total surface area.

The Mn catalyst made using evaporation outperformed the other single metal systems tested by demonstrating over four times greater overall sulfur adsorption, with a break-through occurring at 1410 minutes versus a mere 240 minutes for Mn catalysts made via filtration as shown in Figure 8. These characterization data support this result greatly. The Mn catalyst produced by evaporation had nearly five times the surface area of the filtration sample (43.308 m2/g vs. 10.833 m2/g) along with roughly two-and-a-half times the total pore volume (0.223 cm3/g vs. 0.091 cm3/g). Therefore, it is logical to conclude there were significantly more active adsorption sites available on the evaporation-produced Mn catalyst. Furthermore, SEM imaging demonstrated a more open and fractured morphology for the evaporation-produced Mn catalyst, while XPS analysis indicated a stronger Mn surface signal due to manganese being primarily present as either Mn^{2+}/ Mn^{3+}/ Mn4+oxide. Also, the XRD data indicated the MnOx formed during evaporation was dispersed across the surface more evenly and did not have large crystallites such as those seen in the filtration-produced Mn catalyst. Thus, taken together, the characterization data demonstrate that the increased Mn break-through rate observed in this study was a direct result of a combination of factors including increased Mn retention, increased oxide availability for adsorption, and an optimal surface structure for MnOx adsorption sites. These are consistent with what is known about manganese oxide's ability to bind

 doi:10.20944/preprints202604.0621.v1

sulfur-containing molecules and their redox properties that allow them to use surface-bound oxygen atoms to facilitate additional sulfur binding through adsorption mechanisms [43,44].

The Cu catalyst demonstrated an equally impressive increase in the breakthrough time when comparing the evaporation prepared samples to those prepared using filtration. Specifically, as seen in Figure 8, the evaporation prepared Cu catalyst achieved breakthrough at about 1350 minutes; whereas the Cu catalysts prepared through filtration were able to achieve breakthrough of only 215 minutes. Therefore, the significant increase in the time to reach breakthrough indicates that there was a substantially more effective sulfur adsorbent on the surface of the Cu evaporation catalyst. The data from structural and chemical characterization techniques supported these findings. Specifically, BET analysis showed that evaporation enhanced both the surface area (18.292 m^2/g vs 9.651 m^2/g) and pore volume (0.125 cm^3/g vs 0.076 cm^3/g) of the Cu catalyst. Additionally, SEM images demonstrated a more accessible, roughened morphology for the evaporation prepared sample. Furthermore, XRD showed evidence of more developed CuO related features in the evaporation prepared sample and XPS demonstrated a significantly increased Cu surface signal indicative of oxidized Cu^+/Cu^{2+} species. Finally, EDS demonstrated that a larger amount of Cu was present in the evaporation prepared catalyst compared to its corresponding filtration prepared counterpart, thereby demonstrating that losses of precursors during filtration decreased the quantity of Cu based active sites available for reaction. Consistent with the previous observations, the FTIR results also demonstrate stronger interactions between Cu and O/surface oxygen within the pores of the evaporation prepared catalyst. Overall, it can be concluded that the increased Cu break-through performance of the evaporation prepared catalyst relative to that prepared via filtration is attributed to increased retention of Cu, more developed Cu oxides and increased accessibility of the pore structure.

The evaporation process helped the Zn catalyst as well, although the advantage from evaporation was less in comparison to Mn and Cu, the evaporation-produced Zn catalyst achieved breakthrough of 480 minutes versus 205 minutes for the filtration-produced Zn catalyst. The importance of this increase is furthered due to the fact that the Zn system illustrates that sulfur adsorption does not solely rely on BET surface area. It is true that the evap-oration-produced Zn catalyst had a lower BET surface area (14.034m^2/g) and pore volume (0.096cm^3/g), whereas the filtration-produced Zn catalyst had a higher BET surface area (38.769 m^2/g) and pore volume (0.213cm^3/g). However, when comparing their respective performances, there was substantial improvement in performance for the evaporation-produced Zn catalyst. The evidence indicates that the primary difference between the two Zn samples is that evaporation created a significantly larger mean pore diameter (274.758Å) for the evaporation-produced Zn catalyst in addition to retaining a stronger Zn-surface presence. Additionally, XPS indicated a stronger Zn 2p signal for the evaporation-produced Zn catalyst, suggesting greater Zn^{2+} surface retention of Zn-species. Furthermore, XRD demonstrated more clearly defined ZnO-related peaks for the evaporation-produced Zn catalyst. Lastly, SEM demonstrated an open and brittle structure for the evaporation-produced Zn catalyst. Overall, these findings demonstrate that the increased performance of the Zn-evaporated catalyst were not due to having a larger total BET surface area, but rather better pore-accessibility and a more effective ZnO-rich active surface.

Ni was the least effective of all single metal systems tested; however, the differences among the routes were significant. The evaporation prepared Ni catalyst required 60 minutes to reach a breakthrough point compared to 30 minutes for the filtration route. While the overall effectiveness of Ni was significantly less than that of Mn, Cu and Zn, the evaporation route provided an approximate 2-3 times longer useful life of the catalyst. Again, this demonstrated a superior preservation of the active phase. A higher level of Ni was observed on the surface of the evaporated sample using XPS as evidenced by a slightly greater Ni sur-face signal. XPS also found most of the Ni in the form of Ni^{2+} oxides. XRD found similar levels of NiO related peaks in both samples, with some indication of finer oxide particles formed from the evaporation process. A comparison of SEM images revealed a more porous structure in the evaporation sample. In addition, BET measurements showed a larger average pore diameter (222.430 vs 165.525 Å) in the evaporated sample although it also showed lower values

 doi:10.20944/preprints202604.0621.v1

for total surface area and pore volume. Therefore, these results demonstrate that while accessibility of the active sites and chemical quality of those sites are more important than simply BET surface area, there appears to be some intrinsic limitations based upon the properties of the Ni based oxide surface with respect to sulfur adsorption chemistries under current test conditions.

The evaporation method was very beneficial to the composite catalyst. In comparison to the composite made using the filtration process which achieved breakthrough at approximately 300 minutes, the composite made by evaporation took approximately 480 minutes to achieve breakthrough. Overall better metal retention was evidenced by EDS for the composite made via evaporation. Further, it has been shown by XPS that there were enhanced surface signatures from Zn^{2+}, Cu^{+}/Cu^{2+}, Ni^{2+} and Mn^{2+}/Mn^{3+} species for the composite prepared via evaporation relative to that of the composite prepared using filtration. Further, similar over-lapping mixed-oxide diffraction lines are seen from the two samples; however, there are more defined and similarly dispersed oxide phases present in the evaporation-prepared sample. A higher degree of porosity and fracture was noted for the composite prepared via evaporation. BET analysis provided evidence of higher pore volumes (0.133 vs 0.096 cm^3/g) and larger average pore sizes (241.840 vs 172.030 Å) although a smaller surface area.

The key findings of the study, taken as a whole, have led to an overall mechanistic understanding of the process. The evaporation method produced better performing catalysts because it maintained a greater percentage of active metal precursors attached to the support throughout the synthesis process and permitted them to remain in contact with the support after the solvents had been removed, thus providing conditions favorable to the complete oxidation of the precursor material and its even distribution over the accessible surface areas of the support. In comparison, filtration caused a physical separation of the liquid from the solid prior to complete retention and conversion of the dissolved metal precursors into reactive metal-oxide surface species. Thus, less metal was available at the surface for sulfur adsorption and there existed shorter adsorption lifetimes. These interpretations are heavily reinforced by collective data obtained through the use of EDS, XPS, XRD, SEM, BET, and FTIR methods. One of the major conclusions drawn from this research is that the catalysts exhibiting the greatest sulfur removal efficiencies did not necessarily possess the largest BET surface areas; instead, they were characterized by their most extensive and chemically active metal-oxide surfaces. For example, when comparing the Zn, Ni, and composite systems pre-pared using either evaporation or filtration techniques, it was found that those prepared via evaporation exhibited greater removal efficiencies than those prepared using filtration techniques regardless of whether they possessed higher or lower BET surface areas. Consequently, while geometric areas (i.e., total areas) played a role in determining how much sulfur could be adsorbed onto these materials, it was not the primary determinant. Rather, the effectiveness of each preparation technique in preserving and exposing the metal-oxygen active sites re-sponsible for sulfur capture appeared to determine the overall sulfur removal efficiency.

doi:10.20944/preprints202604.0621.v1

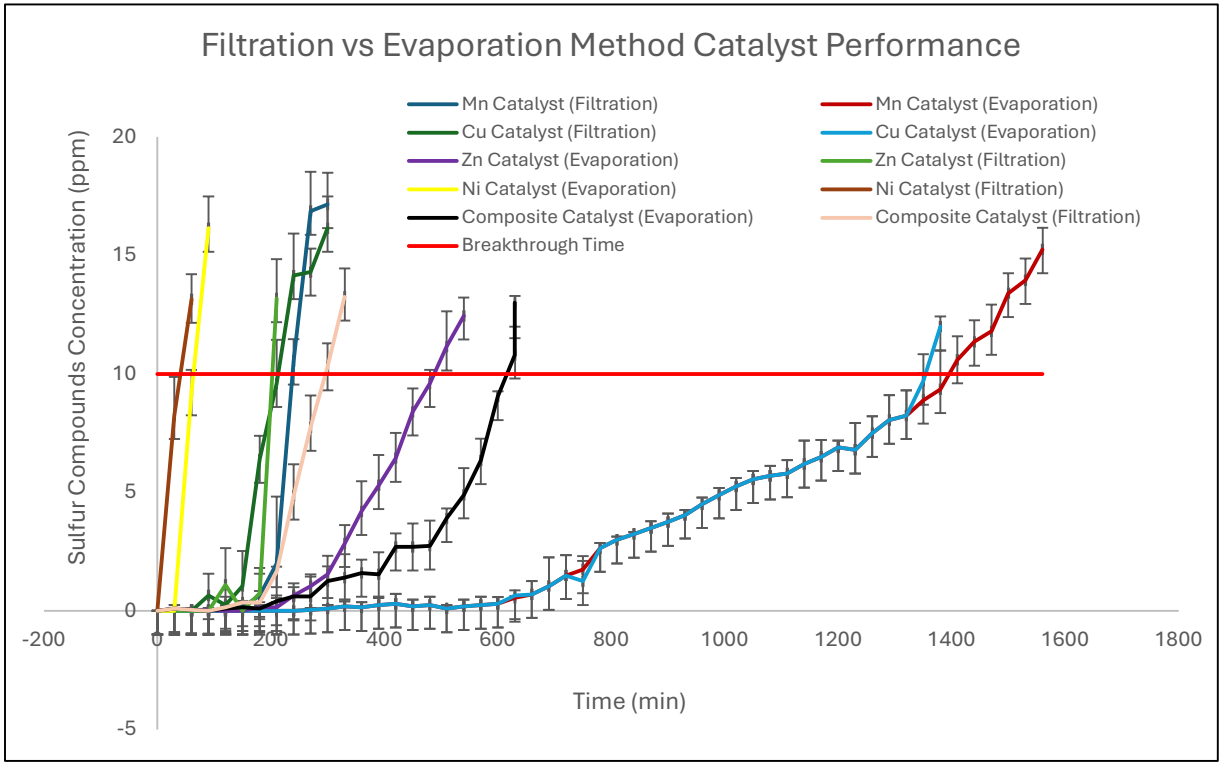

Figure 6. Catalyst Adsorption Performance.

 doi:10.20944/preprints202604.0621.v1

Evaporation-derived Mn and Cu catalysts outperformed commercially available catalyst. Under equivalent experimental conditions, manganese and copper catalysts were able to achieve longer breakthrough times than commercially available as shown in **Figure 7 and Table 2**. Manganese and Copper catalysts achieved longer breakthrough times of 1410 minutes and 1350 minutes respectively in comparison to a commercial catalyst breakthrough time of 1200 minutes. In terms of percentage increase over the commercially available benchmark, Mn catalysts increased breakthrough time by 17.5%, while Cu catalysts had an increase of 12.5%. Commercially available catalyst also showed less ability to adsorb sulfur than Mn and Cu evaporation catalysts. Adsorbed amount of sulfur on a mass basis for commercially available catalyst was 16848 mg/g. Mn and Cu catalysts demonstrated the ability to adsorbed more sulfur prior to becoming exhausted at amounts of 19796.4 mg/g and 18954 mg/g respectively.

Table 2. The Performance Summary the Best Catalysts and the Commercial Catalyst.

Catalyst	Breakthrough Time (minutes)	% change	Sulfur Capacity, q (mg S/g)
Commercial	1200	0%	16848
Mn	1410	17.5%	19796.4
Cu	1350	12.5%	18954

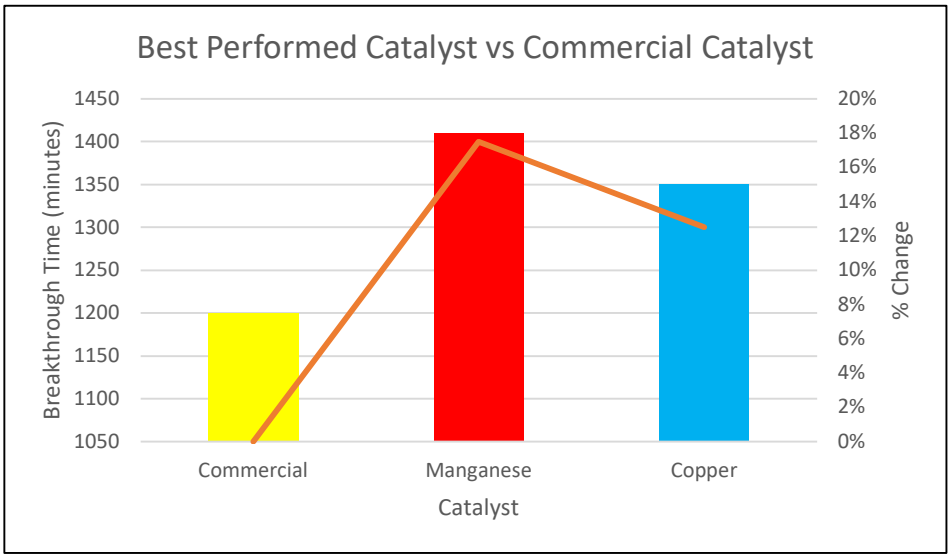

Figure 7. Performance Comparison of the Prepared Catalysts (Evaporation Method) and the Commercial Catalyst.

The findings represent a significant development in terms of practical application since the enhanced performance resulted from an easy-to-implement and cost-effective synthesis process based on solvent evaporation and calcination. The use of solvent evaporation and calcination represents a significantly simpler and less expensive approach to manufacturing catalysts compared to many current commercial methods used in the manufacture of catalysts for industrial applications. Therefore, the Mn and Cu catalysts made with the evaporation method exhibit great promise as economical and scalable substitutes for commercially available catalyst for trace sulfur removal from natural gas streams. Additionally, longer breakthrough times and greater sulfur capacity in industrial fixed bed desulfurization processes would be beneficial since longer catalyst service lives could result in less frequent replacement, increased reliability in fixed bed operations, and better protection for downstream sulfur sensitive equipment.

 doi:10.20944/preprints202604.0621.v1

3. Materials and Methods

3.1. Materials

The chemicals used in the experiments include zinc acetate dihydrate (97%), nickel (II) acetate tetrahydrate (99%), copper (II) nitrate trihydrate (99%), manganese acetate tetrahydrate (98%). Additional reagents include sodium hydroxide and 200-proof ethanol. All chemicals were purchased from Fisher Scientific, except the halloysite pure (support) which was purchased from coastal chemicals in Louisiana, USA. The use of halloysite as a catalyst support is based on the unique naturally occurring aluminosilicate nanotubular structure that provides both an external siloxane surface (Si-O-Si), and an internal aluminol lumen (Al-OH). The unique combination of physical and chemical properties exhibited by halloysite make it a logical choice for the design of highly efficient metal-oxide catalysts for the removal of sulfur-containing compounds from natural gas [10].

3.2. Catalyst Preparation

All chemicals were of reagent-grade quality and used without further purification. The catalysts prepared in this study as shown in **Figure 8** were made through wet impregnation-reflux technique. This process is intended to provide an even distribution of metal oxides over the halloysite surface and at the same time retain the physical properties of the halloysite. Raw halloysite was first crushed and sifted with a 40-mesh sieve to create particles that averaged about 0.4mm in diameter. Halloysite weighing a total of 3g was then mixed in 120mL of 99.5% ethanol to make a homogeneous solution (solution 2) for sonication. Sonication is widely reported to improve dispersion of metal precursors on porous supports by reducing particle agglomeration, enhancing interfacial contact, and promoting more uniform deposition of active species [11,12].

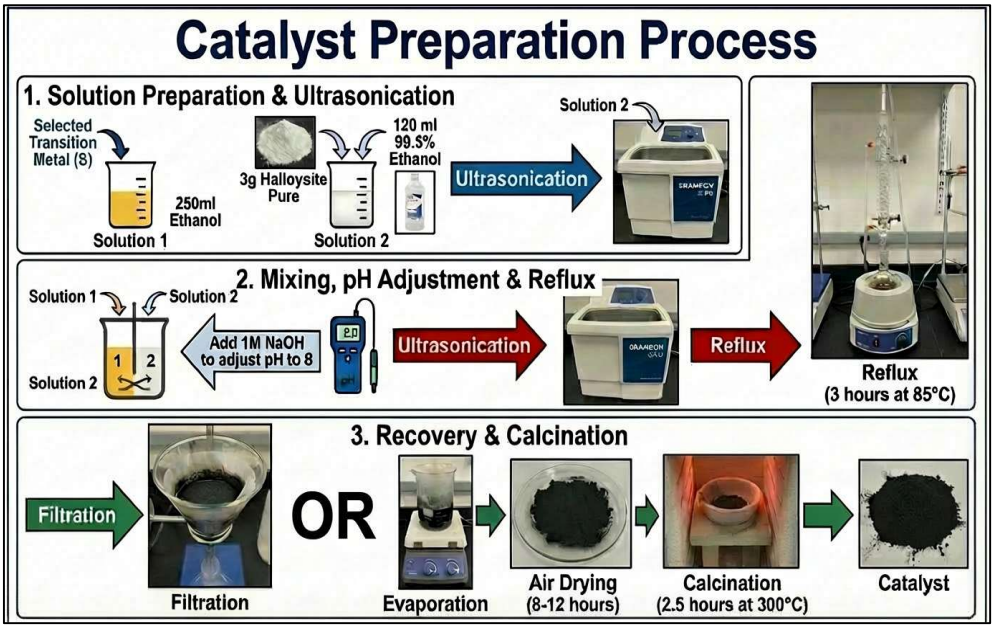

Figure 8. Catalyst Preparation Methods.

A separate precursor solution for transition metals was prepared by dissolving selected metal(s) in 240 ml of 99.5% ethanol. To create Solution 1, the appropriate in-dividual metal salt(s) (Zn, Cu, Mn, Ni) for the particular catalyst formulation were added. The amount of metal salt(s) added to Solution 1 as shown in Figure 1 was determined from the desired metal loading and weight percent metal content. Since ethanol can effectively dissolve metal precursors without excessive pre-hydrolysis of the metal precursors and allows for control over the rate of metal deposition onto the

 doi:10.20944/preprints202604.0621.v1

alumina support, ethanol was chosen as the solvent [13]. Once Solution 1 had been formed, it was slowly added to Solution 2 and adjusted the pH of the combined solution to approximately 8 with 1 molar NaOH. By maintaining an alkaline environment, conditions are created that allow for the precipitation of metal hydroxide intermediate compounds. These metal hydroxide intermediate compounds are transformed into metal oxide materials upon reflux and calcination. The addition of NaOH as a precipitation agent has long been recognized as effective in promoting the immobilization of metal species onto aluminosilicate support via electrostatic forces and by providing sites for nucleation of metal species at surface hydroxyl groups [13]. Following the mixing of the two solutions, it was ultrasonically dispersed to facilitate uniform distribution of metal species throughout the internal pore volume of the halloysite mineral. The suspension was then refluxed at 85 °C for 3 hours to enable deposition and reaction of the metal species with the support. Refluxing facilitates the diffusion of metal ions into the halloysite lumen and aids in creating a strong metal-support bond; these bonds are essential to the stability of the catalyst [14]. After reflux, the resulting solids were removed from the liquid phase via filtration or evaporation method. The solids were dried under air for 8-12 hours and then calcined at 300 °C for 2.5 hours. The calcination process converts the metal hydroxide species that have been deposited on the support into their respective metal oxides. Additionally, the calcination process stabilizes the structural framework of the catalyst. The calcination process is conducted at a relatively low temperature as it enables the production of the necessary metal oxides and minimizes the sintering of the metal particles thereby maintaining the surface area of the support [15].

3.3. Catalyst Testing Process

The catalytic activity test as shown in **Figure 9** was carried out in a stainless-steel tube packed bed reactor with dimensions of 310 mm in length and an inner diameter of 6.35 mm. In each experimental run, 0.5 g of catalyst was loaded in the reactor with the help of glass wool to keep it in place. After loading, the reactor bed was pressured at 60 psi with a nitrogen gas flow rate of 36 mL/min. Once the operational pressure was attained, the system was leak tested using Snoop TM and then left for 30 minutes to see if there were any minor leaks that Snoop TM did not detect by measuring the pressure drop on the pressure gauge. This enabled for leak testing of all connections, from the gas tank to the downstream mass flow controller. Once the system was found to be leak-free, to start the sulfur compounds removal process, the feed was changed from N_2 to a gas mixture with 200 ppm ethyl mercaptan in methane. The gas combination was introduced axially into the packed bed reactor at 25^0C, 200psi and 36 mL/min. Once the flow was stabilized at the proper pressure, the GC-MS procedure began immediately. Breakthrough data was collected once breakthrough (10ppm) attained. A breakthrough concentration of 10 ppm (5% of initial concentration of sulfur in the natural gas used in this experiment) was selected, which is below typical U.S. pipeline sulfur limits (16-20 ppm total sulfur), while remaining within the reliable detection range of the GC-MS and consistent with values reported in desulfurization studies [16,17]. The sulfur capacity of each experiment at breakthrough (q), used to evaluate and compare the results across experimental runs, was calculated using equation (1).

 doi:10.20944/preprints202604.0621.v1

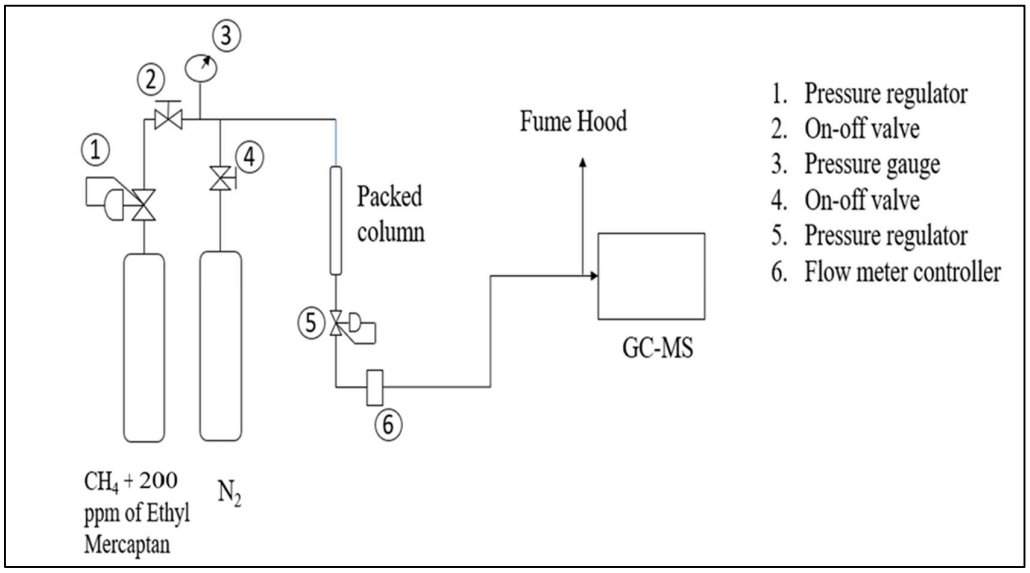

Figure 9. Catalyst Adsorption Performance Experimental Setup.

Ci is the initial concentration of CH_3CH_2SH, C_f is the concentration of the outlet gas, including CH_3CH_2SH, $CH_3CH_2SSCH_3CH_2$, $CH_3CH_2SCH_3CH_2$, in ppm, Q denotes the volumetric flow rate of the model gas, measured in mL/min, t corresponds to the breakthrough time, measured in minutes, M indicates the mass of the loaded catalyst and f is a correction factor that accounts for deviations from ideal plug-flow behaviour, including gas compressibility, pressure effects, and sulphur speciation in the outlet stream, in this study, was taken as unity under steady state conditions

$$q = \left(\frac{Q}{M}\int_0^t (C_i - C_f)dt\right) * f \quad (1)$$

4. Conclusions

1. The catalyst preparation route was shown to be a critical factor controlling sulfur adsorption performance, with the evaporation method consistently outperforming filtration due to improved retention and utilization of active metal species on the support.
2. Evaporation preserved a higher concentration of surface-accessible metal oxides, as confirmed by EDS and XPS, enabling stronger metal-oxygen active sites that enhanced interaction with sulfur-containing molecules.
3. Structural characterization (SEM and BET) revealed that evaporation produced a more porous, rough, and accessible morphology, which improved gas diffusion and exposure of active sites, even in cases where total BET surface area was not maximized.
4. Phase and dispersion analysis (XRD) indicated that evaporation promoted better developed and more finely distributed metal oxide phases, while filtration led to reduced oxide presence and less effective surface coverage due to precursor loss.
5. The Mn and Cu catalysts prepared via evaporation exceeded the performance of the commercial catalyst, achieving longer breakthrough times and demonstrating that simple synthesis control can yield materials with commercially competitive or superior adsorption performance.
6. Overall, the evaporation route provides a scalable, low-complexity, and effective strategy for producing high-performance halloysite-supported metal oxide catalysts, with strong potential for industrial natural gas desulfurization applications, particularly for the removal of trace sulfur compounds such as ethyl mercaptan.
7. The evaporation-prepared Mn and Cu catalysts outperformed the commercial catalyst under identical test conditions, achieving longer breakthrough times (1410 min for Mn and 1350 min for Cu vs. 1200 min for the commercial catalyst) and higher calculated sulfur capacities,

 doi:10.20944/preprints202604.0621.v1

demonstrating that a simple and scalable preparation route can yield low-cost catalysts with strong potential for fixed-bed natural gas desulfurization applications.

Author Contributions: Conceptualization, R.H. and M.E.Z.; methodology, R.H., M.E.Z., and S.A.; formal analysis, R.H., S.A., and W.E.H.; data curation, S.A, D.C and W.E.H ; writing-original draft preparation, S.A. writing-review and editing, R.H., M.E.Z., S.A., D.F., T.K., A.G., and E.R.; project administration, R.H, M.E.Z, and W.E.H.; funding acquisition, R.H and M.E.Z. All authors have read and agreed to the published version of the manuscript.

Funding: This research was supported by the Guangdong Basic and Applied Basic Research Foundation (no. 2021A1515012342) U.S.–Israel Fossil Energy Center (FEC19) administered by the BIRD Foundation and funded by the Israeli Energy Ministry and the U.S. Department of Energy.

Data Availability Statement: All data have been provided in the manuscript.

Acknowledgments: The authors acknowledge the financial support of the U.S. - Israel Fossil Energy Center (FEC19) administered by the BIRD Foundation and funded by the Israeli Energy Ministry and the U.S. Department of Energy for this work.

Conflicts of Interest: All Authors declare that there is no conflict of interest regarding the manuscript.

References

1. Taheri, A., Babakhani, E.G. and Towfighi, J., 2017. Methyl mercaptan removal from natural gas using MIL-53 (Al). Journal of Natural Gas Science and Engineering, 38, pp.272-282.
2. Zhao, H., Hu, L., Zhang, X., Zhu, J. and He, J., 2022. Adsorption and separation of ethyl mercaptan from methane gas on Ni–Ti–LDH nanosheets. Applied Physics A, 128(8), p.687.
3. Castro, P.S., Zuniga, G.M., Holmes, W., Buchireddy, P.R., Gang, D.D., Revellame, E., Zappi, M. and Hernandez, R., 2023. Review of the adsorbents/catalysts for the removal of sulfur compounds from natural gas. Gas Science and Engineering, 115, p.205004.
4. Xie, Y., Bao, J., Song, X., Sun, X., Ning, P., Wang, C., Wang, F., Ma, Y., Fan, M. and Li, K., 2023. Catalysts for gaseous organic sulfur removal. Journal of hazardous materials, 442, p.130029.
5. Aminuddin, M.S., Bustam, M.A. and Johari, K., 2024. Latest technological advances and insights into capture and removal of hydrogen sulfide: a critical review. RSC sustainability, 2(4), pp.757-803.
6. Pinna, F., 1998. Supported metal catalysts preparation. Catalysis Today, 41(1-3), pp.129-137.
7. Lekhal, A., Glasser, B.J. and Khinast, J.G., 2001. Impact of drying on the catalyst profile in supported impregnation catalysts. Chemical engineering science, 56(15), pp.4473-4487.
8. Regalbuto, J. ed., 2016. Catalyst preparation: science and engineering. CRC press.
9. Van Dillen, A.J., Terörde, R.J., Lensveld, D.J., Geus, J.W. and De Jong, K.P., 2003. Synthesis of supported catalysts by impregnation and drying using aqueous chelated metal complexes. Journal of Catalysis, 216(1-2), pp.257-264.
10. Joussein, E., Petit, S., Churchman, J., Theng, B., Righi, D. and Delvaux, B.J.C.M., 2005. Halloysite clay minerals—a review. Clay minerals, 40(4), pp.383-426.
11. Suslick, K.S., 1990. Sonochemistry. science, 247(4949), pp.1439-1445.
12. Suslick, K.S. and Price, G.J., 1999. Applications of ultrasound to materials chemistry. Annual Review of Materials Science, 29(1), pp.295-326.
13. Busca, G., 2014. Heterogeneous catalytic materials.
14. Du, M., Guo, B. and Jia, D., 2010. Newly emerging applications of halloysite nanotubes: a review. Polymer International, 59(5), pp.574-582.
15. Trovarelli, A. and Fornasiero, P., 2013. catalysis. by ceria and related materials London, (12), pp.1-888.
16. Winston, D. and Ariaratnam, S.T., 2022. Navigating Federal and State HDD Guidelines for Interstate Natural Gas Pipeline Crossings. Journal of Pipeline Systems Engineering and Practice, 13(2), p.04022008.
17. Babich, I.V. and Moulijn, J.A., 2003. Science and technology of novel processes for deep desulfurization of oil refinery streams: a review☆. Fuel, 82(6), pp.607-631.

 doi:10.20944/preprints202604.0621.v1

18. Sing, K.S.W., 1967. Adsorption, surface area, and porosity. Academic press.
19. Rouquerol, J., Rouquerol, F., Llewellyn, P., Maurin, G. and Sing, K., 2013. Adsorption by powders and porous solids: principles, methodology and applications. Academic press.
20. Liu, X., Khinast, J.G. and Glasser, B.J., 2008. A parametric investigation of impregnation and drying of supported catalysts. Chemical Engineering Science, 63(18), pp.4517-4530.
21. Munnik, P., De Jongh, P.E. and De Jong, K.P., 2015. Recent developments in the synthesis of supported catalysts. Chemical reviews, 115(14), pp.6687-6718.
22. Yang, R.T., 2003. Adsorbents: fundamentals and applications. John Wiley & Sons.
23. Zuniga, G.M., 2023. Developing Catalysts for the Removal of Methyl Mercaptan from Natural Gas. University of Louisiana at Lafayette.
24. Yuan, P., Southon, P.D., Liu, Z., Green, M.E., Hook, J.M., Antill, S.J. and Kepert, C.J., 2008. Functionalization of halloysite clay nanotubes by grafting with γ-aminopropyltriethoxysilane. The Journal of Physical Chemistry C, 112(40), pp.15742-15751.
25. Frost, R.L. and Vassallo, A.M., 1996. The dehydroxylation of the kaolinite clay minerals using infrared emission spectroscopy. Clays and Clay minerals, 44(5), pp.635-651.
26. Vallarino, L.M., 1991. Macrocyclic complexes of the lanthanide (III), yttrium (III) and dioxouranium (VI) ions from metal-templated syntheses. Handbook on the physics and chemistry of rare earths, 15, pp.443-512.
27. Farmer, V.C., 1974. The Infrared Spectra of Minerals. Mineralogical society monograph, 4, pp.331-363.
28. Mehrabadi, B.A., Eskandari, S., Khan, U., White, R.D. and Regalbuto, J.R., 2017. A review of preparation methods for supported metal catalysts. Advances in catalysis, 61, pp.1-35.
29. Arenas, L.T., Simm, C.W., Gushikem, Y., Dias, S.L., Moro, C.C., Costa, T.M. and Benvenutti, E.V., 2007. Synthesis of silica xerogels with high surface area using acetic acid as catalyst. Journal of the Brazilian Chemical Society, 18(5), pp.886-890.
30. Yuan, P., Tan, D. and Annabi-Bergaya, F., 2015. Properties and applications of halloysite nanotubes: recent research advances and future prospects. Applied Clay Science, 112, pp.75-93.
31. Theng, B.K., 2024. The chemistry of clay-organic reactions. CRC Press.
32. Goldstein, J.I., Newbury, D.E., Michael, J.R., Ritchie, N.W., Scott, J.H.J. and Joy, D.C., 2017. Scanning electron microscopy and X-ray microanalysis. springer.
33. Bartholomew, C.H. and Farrauto, R.J., 2011. Fundamentals of industrial catalytic processes. John Wiley & Sons.
34. Cavani, F., Trifiro, F. and Vaccari, A.J.C.T., 1991. Hydrotalcite-type anionic clays: Preparation, properties and applications. Catalysis today, 11(2), pp.173-301.
35. Westmoreland, P.R. and Harrison, D.P., 1976. Evaluation of candidate solids for high-temperature desulfurization of low-Btu gases. Environmental Science & Technology, 10(7), pp.659-661.
36. Flytzani-Stephanopoulos, M., Gavalas, G.R., Tamhankar, S.S. and Sharma, P.K., 1984. Novel sorbents for high temperature regenerative H2S removal. United States Department of Energy.
37. Biesinger, M.C., Payne, B.P., Grosvenor, A.P., Lau, L.W., Gerson, A.R. and Smart, R.S.C., 2011. Resolving surface chemical states in XPS analysis of first row transition metals, oxides and hydroxides: Cr, Mn, Fe, Co and Ni. Applied Surface Science, 257(7), pp.2717-2730.
38. Di Castro, V. and Polzonetti, G., 1989. XPS study of MnO oxidation. Journal of Electron Spectroscopy and Related Phenomena, 48(1), pp.117-123.
39. Ilton, E.S., Post, J.E., Heaney, P.J., Ling, F.T. and Kerisit, S.N., 2016. XPS determination of Mn oxidation states in Mn (hydr) oxides. Applied Surface Science, 366, pp.475-485.
40. Poulston, S., Parlett, P.M., Stone, P. and Bowker, M., 1996. Surface oxidation and reduction of CuO and Cu2O studied using XPS and XAES. Surface and Interface Analysis: An International Journal devoted to the development and application of techniques for the analysis of surfaces, interfaces and thin films, 24(12), pp.811-820.
41. Van der Heide, P., 2011. X-ray photoelectron spectroscopy: an introduction to principles and practices. John Wiley & Sons.

 doi:10.20944/preprints202604.0621.v1

42. Grosvenor, A.P., Biesinger, M.C., Smart, R.S.C. and McIntyre, N.S., 2006. New interpretations of XPS spectra of nickel metal and oxides. Surface science, 600(9), pp.1771-1779.
43. Wang, P., Zhang, S., Wang, Z., Mo, Y., Luo, X., Yang, F., Lv, M., Li, Z. and Liu, X., 2023. Manganese-based oxide electrocatalysts for the oxygen evolution reaction: a review. Journal of Materials Chemistry A, 11(11), pp.5476-5494.
44. Li, S., Zhang, B., Yang, Y., Zhu, F., Zhao, D., Shi, S., Wang, S., Ding, S. and Chen, C., 2024. Insights into the Acidic Site in Manganese Oxide in Terms of the Sulfur and Water Tolerance of Low-Temperature NH3 Selective Catalytic Reduction. Langmuir, 40(28), pp.14504-14514.